BIBLIOGRAPHIC DATA SHEET

1. CONTROL NUMBER: PN-AAJ-016
2. SUBJECT CLASSIFICATION (695): AF12-0000-0000

3. TITLE AND SUBTITLE (240)

Summary of skimming well investigations

4. PERSONAL AUTHORS (100)

McWhorter, D.B.

5. CORPORATE AUTHORS (101)

Colo. State Univ. Engineering Research Center

6. DOCUMENT DATE (110): 1980
7. NUMBER OF PAGES (120): 87p.
8. ARC NUMBER (170): 628.11.M177

9. REFERENCE ORGANIZATION (130)

Colo. State

10. SUPPLEMENTARY NOTES (500)

(In Water management technical rpt. no. 63)

11. ABSTRACT (950)

This report summarizes the theoretical, laboratory, and field research conducted as part of the Water Management Research Project at Colorado State University. The research was specifically oriented toward Pakistan problems but much of the material is more generally applicable. Salt water upconing in isotropic and anisotropic aquifers beneath wells was examined using both laboratory and numerical models, and guidelines for the construction and operation of wells to minimize contamination by upconing are provided. A method for determining the maximum safe depth of drains below the water table is also provided.

12. DESCRIPTORS (920)

Wells
Mathematical models
Construction
Laboratory equipment
Drainage
Pakistan
Skimming
Field tests
Salinity
Tubewells

13. PROJECT NUMBER (150): 931048900

14. CONTRACT NO.(140): AID/ta-C-1411

15. CONTRACT TYPE (960): Res.

16. TYPE OF DOCUMENT (960)

628 11
M177

SORTIUM FOR RNATIONAL DEVELOPMENT

PN-AAJ-014

Colorado State University
University of Arizona
University of California at Davis
and at Riverside
Utah State University
New Mexico State University
Oregon State University
Texas Tech University
University of Idaho
Washington State University

SUMMARY OF SKIMMING WELL INVESTIGATIONS

D. B. McWhorter

Water Management Research Project
Colorado State University
Fort Collins, Colorado

April 1980

SUMMARY OF SKIMMING WELL INVESTIGATIONS

WATER MANAGEMENT TECHNICAL REPORT NO. 63

Prepared under support of
United States Agency for International Development
Contract AID/ta-C-1411.
All reported opinions, conclusions or
recommendations are those of the
authors and not those of the funding
agency or the United States Government.

Prepared by

David B. McWhorter

Water Management Research Project
Engineering Research Center
Colorado State University
Fort Collins, Colorado

April, 1980

WATER MANAGEMENT TECHNICAL REPORTS*

Consortium for International Development

Colorado State University

No.	Title	Author	No. of Pages	Cost
1	Bibliography with Annotations on Water Diversion, Conveyance, and Application for Irrigation and Drainage, CER69-70KM3, Sept. 1969	K. Mahmood A. G. Mercer E. V. Richardson	165	$3.00
**2	Organization of Water Management for Agricultural Production in West Pakistan (a Progress Report) ID70-71-1, May 1970	P.O. Foss J.A. Strayer R. Dildine A. Dwyer R. Schmidt	148	$3.00
3	Dye Dilution Method of Discharge Measurement, CER70-71 WSL-EVR47, January 1971	W.S. Liang E.V. Richardson	36	$3.00
4	Not available			
**5	The Economics of Water Use, An Inquiry into the Economic Behavior of Farmers in West Pakistan, MISC-D-70-71DW44, March 1971	Debebe Worku	176	$3.00
**6	Pakistan Government and Administration: A Comprehensive Bibliography, ID70-71GNJ17, March 1971	Garth N. Jones	114	$3.00
**7	The Effect of Data Limitations on the Application of Systems Analysis to Water Resources Planning in Developing Countries, CED70-71LG35, May 1971	Luis E. Garcia-Martinez	225	$3.00
**8	The Problem of Under-Irrigation in West Pakistan: Research Studies and Needs, ID70-71GNJ-RLA19	G.N Jones R.L. Anderson	53	$3.00
9	Check-Drop-Energy Dissipator Structures in Irrigation Systems, AER70-71, GVS-VTS-WRM4, May 1971	G.V. Skogerboe V.T. Somoray W.R. Walker	180	$3.00
**10	Maximum Water Delivery in Irrigation	J.H. Duke, Jr.	213	$3.00

*Reports are available from Publications Office, Engineering Research Center, Colorado State University, Fort Collins, CO 80523. Price: as indicated until supply is exhausted; subsequent Xerox copies obtainable at 10 cents per page. Postage and handling: $1.00 in the U.S.; $2.00 to foreign addresses.

**Supply exhausted.

No.	Title	Author	No. of Pages	Cost
11	Flow in Sand-Bed Channels	K. Mahmood	292	$3.00
**12	Effect of Settlement on Flume Ratings	T.Y. Wu	98	$3.00
**13	The Problem of Water Scheduling in West Pakistan: Research Studies and Needs, ID71-72GMJ8, November 1971	G.M. Jones	39	$3.00
**14	Monastery Model of Development: Towards a Strategy of Large Scale Planned Change, ID71-72GMJ9, November 1971	G.M. Jones	77	$3.00
**15	Width Constrictions in Open Channels	J.W. Hugh Barrett	106	$3.00
**16	Cutthroat Flume Discharge Relations	Ray S. Bennett	133	$3.00
**17	Culverts as Flow Measuring Devices	Va-son Boorkirc	104	$3.00
18	Salt Water Coning Beneath Fresh Water Wells	Brij Mohan Sahni	168	$3.00
19	Installation and Field Use of Cutthroat Flumes for Water Management	G.V. Skogerboe Ray S. Bennett Wynn R. Walker	131	$3.00
20	Steady and Unsteady Flow of Fresh Water in Saline Aquifers	D.B. McWhorter	51	$3.00
21	Dualism in Mexican Agricultural Development: Irrigation Development and the Puebla Project	H.M. Biggs	28	$3.00
22	The Puebla Project: Progress and Problems	H.M. Biggs	23	$3.00
**23	Pakistan Government and Administration: A Comprehensive Bibliography, Volume No. 3	G.M. Jones	259	$3.00
24	Index for the Eight Near East-South Asia Irrigation Practices Seminars	W.L. Neal C. Stockmyer	58	$3.00
25	A Bibliography and Literature Review of Groundwater Geology Studies in the Indus River Basin	Alfred J. Tamburi	33	$3.00

No.	Title	Author	No. of Pages	Cost
26	Planning Sediment Distribution in Surface Irrigation Systems	Khalid Mahmood	67	$3.00
27	Practical Skimming Well Design	F.A. Zuberi D.B. McWhorter	61	$3.00
28	Physical, Salinity, and Fertility Analyses of Selected Pakistan Soils	W.T. Franklin W.R. Schmehl	29	$3.00
29	Program for Computing Equilibrium Solution Composition in $CaCO_3$ and $CaSO_4$ Systems from Irrigation Water Compositions	Dhanpat Rai W.T. Franklin	42	$3.00
30	Conjunctive Use of Indus Basin Waters--Pakistan: A General Summary of Ph.D. Dissertation	M.T. Chaudhry	37	$3.00
**31	Informational Sources on Water Management for Agricultural Production in Pakistan with Special Reference to Institutional and Human Factors, Volume I Volume II	G.M. Jones A.R. Rizvani M.B. Malik R.F. Schmidt	170 251	$3.00
32	Crop Water Use and Yield Models with Limited Soil Water	H.M. Meghassi	119	$3.00
33	Design of Irrigation Drop Structures	Soon-kuk Kwun	123	$3.00
**34	A Study of Village Organizational Factors Affecting Water Management Decision Making in Pakistan	A.M. Mirza	129	$3.00
35	Village Organizational Factors Affecting Water Management Decision-Making Among Punjabi Farmers	A.M. Mirza D.M. Freeman J.B. Eckert	62	$3.00
36	Organizational Alternatives to Improve On-Farm Water Management in Pakistan	George E. Radosevich	252	$3.00
37	Improving Farm Water Management in Pakistan	Gilbert L. Corey Wayne Clyma	32	$3.00
38	The Importance of Farm Water Management in Pakistan	Wayne Clyma Gilbert L. Corey	28	$3.00

No.	Title	Author	No. of Pages	Cost
39	Irrigation Practices and Application Efficiencies in Pakistan	Wayne Clyma Arshad Ali M.M. Ashraf	36	$3.00
40	Calibration and Application of Jensen-Haise Evapotranspiration Equation	Wayne Clyma M.R. Chaudhry	16	$3.00
41	Plant Uptake of Water From a Water Table	Chaudhry Nuruddin Ahmad	88	$3.00
42	Physical and Socio-Economic Dynamics of a Watercourse in Pakistan's Punjab: System Constraints and Farmers' Responses	M.K. Loudermilk Wayne Clyma Alan C. Early	106	$3.00
43	Water Management Alternatives for Pakistan: A Tentative Appraisal	Jerry Eckert Niel Dimick Wayne Clyma	61	$3.00
44	Water User Organizations for Improving Irrigated Agriculture: Applicability to Pakistan	George E. Radosevich	34	$3.00
45	Watercourse Improvement in Pakistan: Pilot Study in Cooperation with Farmers at Tubewell 56L	CSU Field Party and Mona Reclamation Experimental Staff (Pakistan)	93	$3.00
46	Planning and Implementing Procedures for Contracting Agricultural-Related Research Programs in Low Income Nations	Max K. Loudermilk Wayne Clyma W. Doral Kemper Sidney A. Bowers	46	$3.00
47	A Research-Development Process for Improvement of On-Farm Water Management	Wayne Clyma Max K. Loudermilk Gilbert L. Corey	58	$3.00
48	Farm Irrigation Constraints and Farmers' Responses: Comprehensive Field Survey in Pakistan			
Volume I - Summary		Max K. Loudermilk Alan C. Early David M. Freeman		$5.00
Volume II - Purpose of the Study, Its Significance, and Description of the Irrigation System		Max K. Loudermilk David M. Freeman Alan C. Early		
Volume III - Consequences of the Present Farm Water Management System		Alan C. Early Max K. Loudermilk David M. Freeman		

No.	Title	Author	No. of Pages	Cost
	Volume IV - Major Constraints Confronting Farmers Explaining the Consequent Low Crop Yields	Max K. Lowdermilk David M. Freeman Alan C. Early	250	
	Volume V - Farmer Responses to Major Constraints: Viable Options Under Present Conditions	David M. Freeman Max K. Lowdermilk Alan C. Early	52	
	Volume VI - Appendices	David M. Freeman Max K. Lowdermilk Alan C. Early	319	
	Volumes II through VI are sold as a set only			$20.00
49A	Evaluation and Improvement of Irrigation Systems	Gideon Peri G.V. Skogerboe	92	$3.00
49B	Evaluation and Improvement of Basin Irrigation	Gideon Peri G.V. Skogerboe Donald Morum	179	$6.00
49C	Evaluation and Improvement of Border Irrigation	Gideon Peri Donald Morum G.V. Skogerboe	105	$3.00
50	Factors Affecting Losses from Indus Basin Irrigation Channels	Thomas J. Trout	201	$6.00
	Special Technical Reports			
	Institutional Framework for Improved On-Farm Water Management in Pakistan	Water Management Research Project Staff	88	$3.00
	Recalibration of Small Cutthroat Flumes for Use in Pakistan	G.V. Skogerboe Abbas A. Fiuzat Thomas J. Trout Richard L. Aust	82	$3.00
51	Farm Water Management in Upland Areas of Baluchistan	W.D. Kemper Mazher-ul-Haq Ahmad Saeed	77	$3.00
52	Operational Irrigation Evaluation of Pakistan Watercourse Conveyance Systems	Thomas J. Trout S.A. Bowers	104	$3.00
53	Irrigation and Honor: Cultural Impediments to the Improvement of Local Level Water Management in Punjab, Pakistan	Douglas J. Murrey	61	$3.00

No.	Title	Author	No. of Pages	Cost
54	Constraints on Small Farmers in the Precision Land Leveling Program in the Pakistani Punjab	Raymond Z.M. Renfro	123	$6.00
55	Organizational Problems and Their Consequences to Improved Watercourses in Punjab	Ashfaq Hussain Mirza and Douglas J. Merrey	186	$6.00
56	Watercourse Improvement Research in Pakistan	W. Doral Kemper Wayne Clyma Gaylord V. Skogerboe Thomas J. Trout	107	$6.00
57	Optimization of Lengths of Alternative Watercourse Improvement Programs	John O. Rouse	49	$3.00
58	Watercourse Improvement Manual	Thomas J. Trout W. Doral Kemper	258	$9.00
59	Field Evaluation of Methods for Measuring Basin Irrigation Performance	Satyansu S. Kundu Gaylord V. Skogerboe	135	$6.00
60	Training Manual for Agricultural Water Management Specialists	Edited by Dwayne G. Westfall	700	$9.00
61	Analysis of Basin-Furrow Irrigation	Gideon Peri Gaylord V. Skogerboe		$3.00
62	Matching Cropping Systems to Water Supply Using an Integrative Model	John O. Reuss	208	$6.00
63	Summary of Skimming Well Investigations	David B. McWhorter	89	$3.00

ABSTRACT

This report summarizes the theoretical, laboratory, and field research conducted as part of the Water Management Research Project at Colorado State University. The research was specifically oriented toward Pakistan problems but much of the material is more generally applicable. Salt water upconing in isotropic and anisotropic aquifers beneath wells was examined using both laboratory and numerical models, and quidelines for the construction and operation of wells to minimize contamination by upconing are provided. A method for determining the maximum safe depth of drains below the water table is also provided.

TABLE OF CONTENTS

	Page
ABSTRACT	vii
LIST OF TABLES	ix
LIST OF FIGURES	x
INTRODUCTION	1
THEORETICAL CONSIDERATIONS	3
Miscible Flow Formulation	4
Immiscible Flow Formulation	6
Conditions on the Interface	8
LABORATORY EXPERIMENTS	11
Choice of Porous Medium	11
Choice of Fluids	12
Equipment and Experimental Set-Up	13
Experimental Procedure	17
Summary of Experimental Results	19
MATHEMATICAL MODELS	25
Interface Upconing Beneath a Horizontal Drain	25
Unsteady Unconing Beneath a Pumping Well	31
The Effect of Anisotropy	35
FIELD EXPERIENCES WITH SKIMMING WELLS	48
Summary Results	55
CONSTRUCTION AND OPERATION OF SKIMMING WELLS	72
Construction	72
Operation	73
REFERENCES	76

LIST OF TABLES

Table No.		Page No.
1	Experimental results.	21
2	Results from Wang's theory.	21
3	Results from Muskat's theory	21
4	Measured and predicted critical conditions.	39
5	Salinity profile in Mona Well on Phularwan Farm.	70
6	Salinity in discharge - Mona Well on Phularwan Farm.	71

LIST OF FIGURES

Figure No.		Page No.
1	Discharge end of the laboratory model.	15
2	Recharge end of the model.	16
3	Comparison of theoretical critical discharge with the experimental results.	22
4	Flow toward a drain.	26
5	Idealized flow toward a drain.	26
6	Graphical solution of Equations 37 and 38.	30
7	An example pumping schedule.	32
8	Schematic of the interface elevation corresponding to the pumping schedule shown in Figure 7.	34
9	Definition sketch for upconing of salt water beneath a pumped well.	38
10	Comparison of measured and calculated results for flow to a well in an isotropic aquifer.	40
11	Critical discharge as a function of well penetration.	42
12	Relationship between optimum penetration ratio and permeability ratio.	44
13	Relation between discharge and interface elevation for various permeability ratios.	45
14	Tubewell and observation well layout.	50
15	Salinity profile at skimming well test site.	51
16	Tubewell construction.	53
17	Construction of observation wells.	54
18	Salinity profile of skimming well site.	56
19	Observation well at T1-3.	57

LIST OF FIGURES, continued

Figure No.		Page No.
20	Level of water in tubewell 2 during pumping.	59
21	Water table before, after and during pumping.	60
22	Salinity of water in the aquifer as a function of depth below the surface before and during pumping.	62
23	Salinity of water in the aquifer as a function of depth below the surface and before and during pumping.	63
24	Salinity of water in the aquifer as a function of depth below surface before and during pumping.	64
25	Rise of saline-fresh water interface as indicated by the successive positions of the 5mmho/cm isoconcentration line.	66
26	Salt content of well water which was being pumped at a rate of 225 gallons/minute.	66
27	Fall of saline-fresh water interface following pumping (as indicated by successive positions of 5mmho/cm equal concentration line.	67

SUMMARY OF SKIMMING WELL INVESTIGATIONS

D. B. McWhorter[1]

INTRODUCTION

Exploitation of groundwater supplies for agricultural, municipal and industrial uses is severely hampered in many regions of the world by the encroachment of unusable saline water in response to fresh water withdrawals. Examples of salt water encroachment are most numerous in coastal aquifers but are sometimes present in inland aquifers as well. Probably the most important example of the latter case exists in the India-Pakistan subcontinent in the Indus River Basin.

Pakistan has an area of almost 200 million acres; over 30 million acres of which is irrigated. The irrigated area is laced with thousands of miles of canals and ditches used to supply farmers with essential irrigation water. Seepage from the extensive distribution system and deep percolation from precipitation and irrigation over the years has, in many areas, produced a high water table in the underlying alluvial aquifer. The high water table has caused wide-spread problems of waterlogging and salinity, necessitating the installation of extensive drainage and reclamation programs.

The problem of drainage is complicated by the fact that highly saline water underlies virtually all of the relatively fresh water throughout the aquifer. Near the rivers and

1/Professor, Agricultural and Chemical Engineering Department, Colorado State University, Fort Collins, CO.

canals where a supply of fresh surface water is available, the saline water exists only at great depths. Near the center of the doab between the major tributaries to the Indus a zone of relatively fresh water less than 100 feet thick commonly overlies a zone of more highly saline water (Greenman, et al., 1967). In such areas drainage facilities are apt to draw a substantial portion of their discharge from the saline zone unless special care is taken. The disposal of the saline water produced by such facilities presents a major problem. In many cases the saline water can be discharged into nearby canals or otherwise mixed with canal water and used for irrigation. This procedure can only constitute a short term solution to the problem, however. This fact coupled with the need for supplemental irrigation water provides substantial incentive to "skim" the fresh water from the aquifer with a minimum disturbance of the saline zone.

Over the past several years, Colorado State University has conducted research into the mechanisms of fresh-water flow above a saline zone and investigated procedures for exploiting the fresh water zone without the entrainment of the underlying salt water. This research was initiated with a laboratory model study of salt-water upconing beneath pumping wells. Theoretical studies were also undertaken in which the fresh-salt water system was treated as two zones with distinct densities. Flow in both isotropic and anisotropic aquifers was modeled with the intent of developing design criteria for wells and horizontal drains that would

be capable of skimming the fresh water without substantial entrainment of salt water. Also, a mathematical model was developed that treated the system in terms of flow of a nonhomogeneous fluid. Field experiments were carried out in Pakistan to observe the system behavior under actual conditions and to study the practicality of skimming wells.

This report is a summary of the salient features of the CSU research on flow in fresh-saline water aquifers. It is the intent to provide sufficient background to permit critical assessment of the results without unnecessarily burdening the reader with the details of the procedures.

THEORETICAL CONSIDERATIONS

The complexity of the phenomenon of flow of fresh water underlain by brine has led investigators to make numerous idealizations in attempts to reduce the mathematical description of the phenomenon to a tractable form. A very common practice is to regard the fresh water and brine as immiscible liquids with an abrupt interface between them. In reality the two liquids are miscible and a transition zone separates the brine and the fresh water. The transition zone is characterized by a continuous decrease of concentration of salt from that of the undiluted brine to that of the uncontaminated water above. A mathematical formulation which considers the fluids to be miscible is more realistic but less tractable than one which considers the liquids to be immiscible. Both formulations are important, however, and are discussed in some detail in the following paragraphs.

Miscible Flow Formulation

A discussion of the flow of miscible fluids in porous media requires consideration of hydrodynamic dispersion. Hydrodynamic dispersion is the name given the process by which a contaminant becomes mixed and distributed in a porous medium as the result of velocity distributions and fluctuations and molecular diffusion on a pore-size scale. Mathematical characterization of the phenomenon has required consideration of contaminant transport at the pore-size (microscopic) scale and the development of an averaging procedure by which the microscopic mechanisms can be expressed in macroscopic terms which are observable and measurable. The result is the following equation known as the differential equation of hydrodynamic dispersion:

$$\frac{\partial c}{\partial t} = \frac{\partial}{\partial x_i} \left[D_{i,j} \frac{\partial c}{\partial x_i} - c v_i \right] - S_1 \qquad (1)$$

in which

c = contaminant concentration - M/L^3

t = time - T

x_i = ith cartesian coordinate - L

$D_{i,j}$ = coefficient of hydrodynamic dispersion (a tensor of rank 2) - L^2/T

v_i = the component of seepage velocity in the ith direction - L/T

S_1 = source or sink - $M/L^3 \cdot T$.

Several analytic solutions of the above equation exist under a variety of boundary and initial conditions and with different formulations of the source-sink term (Dagan, 1971; Harleman and Rumer, 1963; Lapidus and Amundson, 1952;

Lindstrom, et al., 1971; Ogata, 1964; Ogata and Banks, 1961). The analytic solutions have contributed greatly to the understanding of hydrodynamic dispersion and their importance cannot be overemphasized. However, the analytic solutions are ordinarily derived for boundary and initial conditions that are relatively simple in comparison to the wide variety of situations encountered in the field.

Numerical solutions using finite difference formulations and the finite element method have also been developed. Numerical solutions are usually more general inasmuch as complex boundary and initial conditions can be handled for dispersion in nonisotropic and nonhomogeneous porous media. Numerical solutions are ordinarily less convenient for analysis and design than are analytical solutions. In many cases, however, numerical methods offer the only feasible means of solving the problem.

Because the seepage velocity v_i is present in equation 1, and because the coefficient of hydrodynamic dispersion $D_{i,j}$ depends on v_i, the phenomenon of dispersion is strongly dependent upon the flow of the solution phase. To some extent the bulk flow of the solution phase is also dependent on the concentration distribution of the contaminant. This is true because the contaminant effects the density and viscosity of the solution. The differential equation for flow including the influence of the contaminant can be written as in equation 2,

$$\frac{\partial}{\partial x_i}\left[\frac{\rho k_{xi}}{\mu}\left(\frac{\partial p}{\partial x_i} + \rho g \frac{\partial h}{\partial x_i}\right)\right] = \frac{\partial}{\partial t}(\rho\phi) + S_2 \qquad (2)$$

where

k_{xi} = intrinsic permeability in the x_i direction $-L^2$

P = pressure - F/L^2

g = gravitational constant - L/T^2

h = elevation with respect to an arbitrary datum - L

ρ = density - M/L^3

μ = dynamic viscosity - $F \cdot T/L^2$

ϕ = porosity

S_2 = source or sink - M/L^3T ,

and other symbols are as previously defined. Equations 1 and 2 constitute a system of partial differential equations which describe bulk flow of a liquid and dispersion of a contaminant in that liquid.

Immiscible Flow Formulation

One of the objectives of the study reported herein, is to provide a method for comparing different methods of producing the relatively fresh water with a minimum disturbance of the underlying brine. From an academic standpoint, the ideal way to accomplish such a comparison would be to solve equations 1 and 2 simultaneously for each method under consideration. A less rigorous approach involves several idealizations which are discussed in the following paragraphs.

It is often the case that the disperse (or transition) zone between the fresh-water region and the salt-water region is small compared to the total thickness of the fresh-water region. It is, therefore, possible to consider the transition zone as a sharp boundary separating the two regions of flow.

The problem is reduced to locating the interface between the two regions for various boundary conditions which is often called a "free-surface" problem.

Within each region separated by the abrupt interface, the flow is given by Darcy's law in vector notation for isotropic media:

$$\vec{q}_f = - K_f \nabla \, (P_f/\gamma_f + z) \tag{3}$$

$$\vec{q}_s = - K_s \nabla \, (P_s/\gamma_s + z) \tag{4}$$

in which

$\vec{q}$ = Darcy velocity vector - L/T

K = hydraulic conductivity - L/T

P = pressure - F/L^2

z = elevation relative to an arbitrary datum - L

γ = specific weight - F/L^3 ,

and the subscripts f and s refer to fresh and salt water respectively. The quantity in parentheses is called the hydraulic head. Throughout the remainder of this report the hydraulic head is denoted by the symbol H. For a homogeneous medium, equation 3 can be combined with the equation for mass conservation for incompressible, homogeneous fluids to obtain:

$$\nabla^2 H_f = 0 \tag{5}$$

The same equation applies to the salt-water region with the subscript f replaced by s. Equation 5 is known as the Laplace equation. The hydraulic head H_f is a function of space and time in general.

The problem is to solve the linear Laplace equation in the fresh water region subject to the boundary conditions. Dagan (1964) has shown that the problem represented by equation 5 within a region whose boundary is partially a free surface is nonlinear because of a nonlinear boundary condition on the interface. The nonlinear boundary condition constitutes the major difficulty with the immiscible formulation of the problem.

Conditions on the Interface

At any point the pressure must be continuous across the interface. Therefore, solving for pressure from the definitions of hydraulic head in the fresh and salt water regions and equating at the interface yields:

$$H_f^{\,i}\,\gamma_f - \xi\gamma_f = H_s^{\,i}\,\gamma_s - \xi\gamma_s \tag{6}$$

in which ξ is the vertical coordinate of the interface at any point, the superscript i denotes the value of hydraulic head on the interface, and other symbols are as previously defined.

Solving equation 6 for the elevation of the interface yields

$$\xi = \frac{\gamma_s}{\Delta\gamma} H_s^{\,i} - \frac{\gamma_f}{\Delta\gamma} H_f^{\,i} \tag{7}$$

in which $\Delta\gamma$ is $\gamma_s - \gamma_f$. Equation 7 implies that the position of the interface can be computed if the values of hydraulic head are known on the interface.

The change in elevation of the interface with respect to the distance along the interface is obtained from equation 7 by differentiation:

$$\frac{\partial \xi}{\partial \ell} = \frac{\gamma_s}{\Delta\gamma}\frac{\partial H_s{}^i}{\partial \ell} - \frac{\gamma_f}{\Delta\gamma}\frac{\partial H_f{}^i}{\partial \ell} \tag{8}$$

where ℓ is the distance along the interface. Solving equations 3 and 4 for the gradient of head and substituting into equation 8 results in

$$\frac{\partial \xi}{\partial \ell} = \frac{\gamma_f}{\Delta\gamma}\frac{q_f{}^i}{K_f} - \frac{\gamma_s}{\Delta\gamma}\frac{q_s{}^i}{K_s} \tag{9}$$

where $q_f{}^i$ and $q_s{}^i$ are the velocities tangent to the interface. The derivative on the left of equation 9 is the slope of the interface and can be replaced by $\sin\theta$ where θ is the angle the interface makes with the horizontal.

The hydraulic conductivities K_f and K_s are directly proportional to the specific weights γ_f and γ_s respectively. Therefore, if it is assumed that the viscosity of the salt and fresh waters are the same, equation 9 implies that, when

$$q_f{}^i = q_s{}^i \ , \tag{10}$$

the interface is horizontal. A horizontal interface also results when there is no flow in either region.

The case in which there is flow in the fresh water but no flow in the salt water is of particular interest. Equation 9 reduces to

$$\frac{\gamma_f q_f{}^i}{\Delta\gamma K_f} = \sin\theta \tag{11}$$

The right side of equation 11 has a maximum value of unity. Therefore, the condition

$$q_f^{\,i} < \frac{\Delta\gamma K_f}{\gamma_f} \tag{12}$$

must be satisfied at all points on the interface. Condition 12 can be regarded as a necessary condition for a static salt water phase. The above condition is quite restrictive because it implies that the fresh water velocity tangent to the interface must remain much less than the value of hydraulic conductivity. This further implies that the hydraulic gradient on the interface must remain less than $\Delta\gamma/\gamma_f$.

The classical Ghyben-Herzberg relation can be stated

$$\Delta\xi = -\frac{\gamma_f}{\Delta\gamma}\,\Delta h \quad , \tag{13}$$

where h is the water table elevation relative to some datum. The Ghyben-Herzberg relation states that the change in elevation of the interface associated with a change in water table elevation is approximately $\Delta\gamma/\gamma_f$ times as great as the water table change. The approximation necessary to arrive at equation 13 follows directly from equation 8 with $\partial H_s^{\,i}/\partial\ell = 0$:

$$\Delta\xi = \frac{\partial\xi}{\partial\ell}\,\Delta\ell = -\frac{\gamma_f}{\Delta\gamma}\,\frac{\partial H_f^{\,i}}{\partial\ell}\,\Delta\ell \ , \tag{14}$$

or

$$\Delta\xi = -\frac{\gamma_f}{\Delta\gamma}\,\Delta H_f^{\,i} \quad . \tag{15}$$

Equation 15 is identical to the Ghyben-Herzberg relation provided the hydraulic head on the interface is equal to the water table elevation. Such a condition exists only if the

flow is horizontal. Therefore, use of the Ghyben-Herzberg relation is tantamount to neglecting the vertical component of flow.

LABORATORY EXPERIMENTS

The laboratory experiments reported herein were conducted by Sahni (1972), and much of the material is taken directly from his dissertation. The purpose of conducting the experimental work was to 1) increase the understanding of the upconing problem, 2) check the validity of the Wang (1965) and Muskat and Wyckoff (1935) theories and 3) to provide data suitable for checking the validity of numerical models. In these experiments, the fresh-salt water system was simulated by two fluids separated by an interface. Thus, no information on the effects of dispersion was obtained.

Choice of Porous Medium

Since capillary forces in the field situation are considered to have negligible effect, an attempt was made to insure that this was the case for the model also. It is difficult to satisfy the requirement for negligible capillary phenomena in designing a laboratory model of practical size. It was necessary to select a material to simulate the aquifer such that the capillary fringe in the model would be only a small fraction of the total thickness of the fresh-water zone. After running several tests with different kinds of materials, it was decided that the simulating material should have an average grain size of at least 2 mm. Since the present study

relates to homogeneous and isotropic aquifers, it was decided to use spherical glass beads about 2.5 mm size.

The glass beads used as the aquifer material in the model, in contrast to soils and sands, could easily be packed to practically the same density in each run. Therefore, it was possible to obtain reproducible results. Another reason for the selection of glass beads as the aquifer material in the model was that their smooth surfaces made it easy to wash them after each experiment. Thus, the same glass beads could be used in all the experiments.

Choice of Fluids

The two fluids in the prototype are fresh water and saline water, which are miscible. As explained before, in actual field conditions a zone of dispersion exists at the contact of the two fluids. This zone, however, may often be a small fraction of the total thickness of the aquifer and therefore, as a simplification in analysis, could be considered as an abrupt interface. When tap water and water with some salt dissolved in it were used in a test model, it was observed that the dispersion zone was a disproportionately large fraction of the total thickness of fresh-water aquifer. Also, because of complete miscibility of the two fluids, this zone of separation was not well defined.

It was also necessary that the amount of mounding of the brine, in response to the production of the well, be a realistic fraction of the total height of the model. A very coarse material was used for the aquifer in the model.

Therefore, if fresh water and saline water had been used, the drawdown in the well would have been very small to keep the mound within realistic limits. However, it was not possible to measure a very small drawdown with the desired accuracy. Further, from equation (13) it was observed that the cone height can be reduced by using two fluids with a larger density contrast.

The above reasons, therefore, led to the choice of two immiscible fluids having a density difference much greater than that for fresh water and saline water. Fresh water was simulated by Soltrol "C" and saline water by tap water containing a dye called Pontacyl. This dye is water soluble and is insoluble in Soltrol. A very small amount of this dye gave a brilliant pink color to water which made visual observation of the interface at various stages of coning quite easy. With this choice of simulating fluids and with careful packing of glass beads in the model it was possible to obtain a well-defined interface between the two fluids.

Equipment and Experimental Set-Up

Ideally, in order to minimize the wall effects on flow, it would be desirable to construct a very large cylindrical model. However, a large model is uneconomical to build, impractical from the point of view of simulating all boundary conditions, and difficult to operate. Since the present work deals with axisymmetrical flow toward a well in a homogeneous and isotropic medium, it was sufficient to construct only a sector of a cylindrical model. The model used in this

study has radial walls forming an angle of 15° which represents 1/24 of a complete cylinder. The radial length of the sector was four feet. Toward the outflow end of the model a brass screen of 50 mesh size was placed at a distance of 0.96 inch from the center line of the cylinder where the gap between the two radial walls of the sector was 1/4 inch. This screen represented the screen of a well of radius 2.38 cm with its axis along the center line of the cylinder. Figure 1 shows the discharge end of the model and Figures 2(a) and 2(b) give details of the recharge end.

The model was made of plexiglass, so that the position of the interface and free surface could be clearly seen. At the inflow end the model was 12.72 inches wide. The total height of the model was two feet. The portion of the model containing the beads was separated at its inflow end from a reservoir by a wall which was perforated uniformly by 63 1/4 inch holes with 2 inch separations. The purpose of this reservoir was to maintain a constant head at the inflow boundary of the model. The liquid level in the reservoir was maintained constant by an overflow tap in the outer wall of the reservoir at a depth of three inches from the top. Perforations at the inner wall insured a uniform distribution of liquid against the outer end of the sector. These holes were covered with a screen to prevent glass beads from falling into the reservoir.

Production from the well was simulated in the model by siphoning oil with a tube (about 1/4 inch I.D.). The height

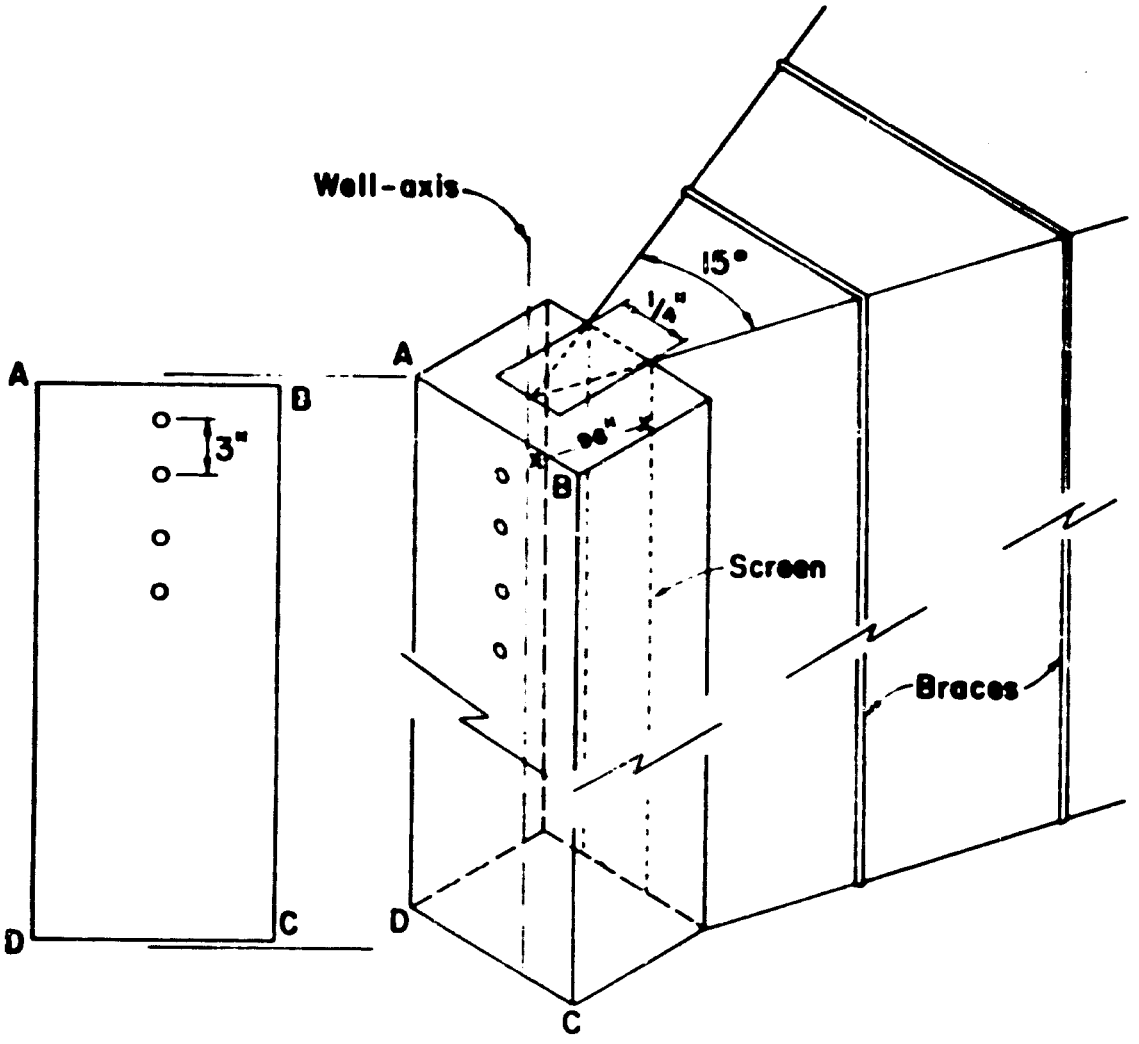

Figure 1. Discharge end of the laboratory model.

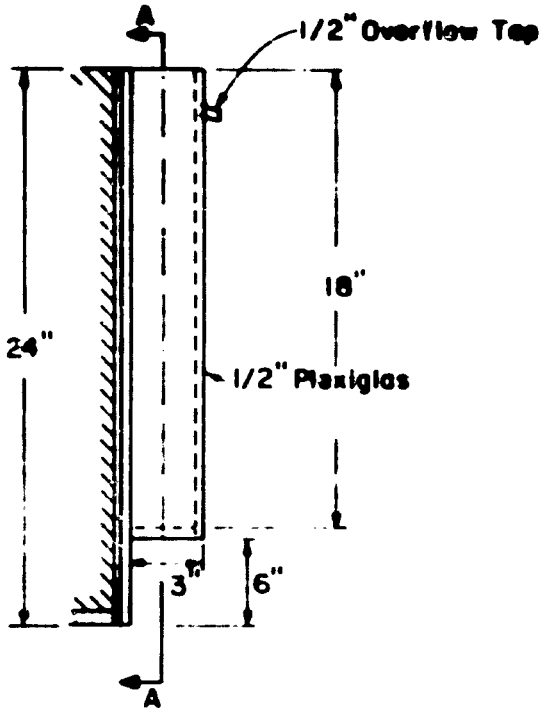

(a) Side View

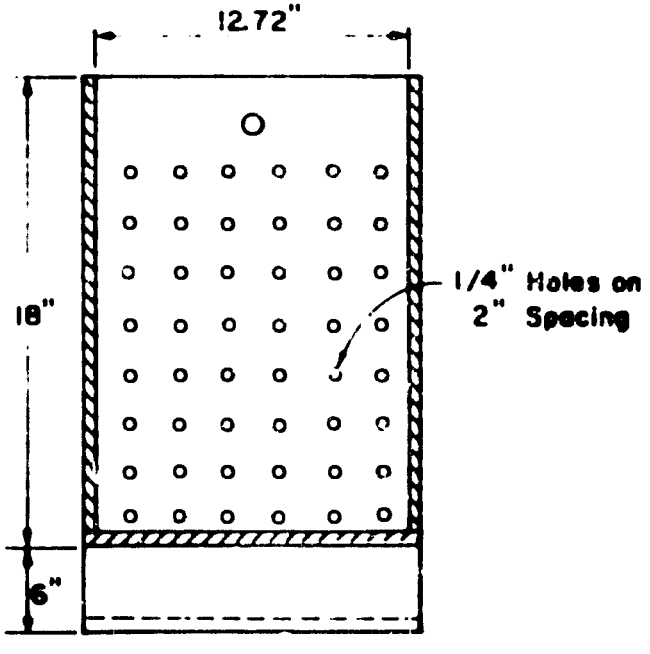

(b) Section A-A

Figure 2. Recharge end of the model.

of the fluid in the well and the production rate were varied with the help of a screw clamp. After allowing sufficient time for the flow to reach an equilibrium following each adjustment of the flow rate, it was possible to maintain a steady flow in the model. Fluid drained from the model was collected in a large measuring jar (about 2 inches in diameter and of 2000 cc capacity), which was provided near its base with an outlet and a stop cock. When the measurements for discharge were not being made, the valve at the outlet of the jar was left open. For making measurements of the producing rate, the valve was closed, so that all the fluid drained by the well was collected in the measuring jar. The flow rate was determined by noting the total volume collected in an increment of time. After the measurement, the stop cock was again opened and the fluid allowed to drain.

Experimental Procedure

Once the model tank was filled with glass beads and fluids, a steady circulation of the fluids was maintained. A reference line was etched on the front wall of the model coinciding with the location of the original free surface. Since in all the experiments, irrespective of the position of the interface, the free surface position prior to pumping was the same, it was convenient to use this line as the reference line rather than the position of the interface. Depths below this reference line were marked in millimeters at a number of suitable distances from the well axis along the front wall and also along the well on the discharge-end plate.

The initial position of the interface and the free surface were noted. Then the production of oil was started at a slow rate. This induced a drawdown of the free surface toward the well in an approximately parabolic shape and an upconing of the interface below the well. In order to insure that the free surface at the recharge end never went below the level of the overflow outlet, the rate of inflow of oil was adjusted so that it was slightly higher than the discharge rate. At the same time, care was taken that the inflow into the reservoir was not high enough to cause ponding at the surface which would result in a higher free surface location at the recharge end than the original position prior to pumping.

After allowing sufficient time for the flow system to reach a steady state, several measurements were made for calculating discharge. The locations of both the free surface as well as the interface were recorded at several radial distances from the well axis. The readings were taken at much closer intervals in the vicinity of the well. This was helpful in making a detailed study of the effects of convergence near the well on the free liquid surface and on production rates.

Next, the discharge was increased and after the flow system had again reached equilibrium under the new conditions, the new discharge was measured and the locations of the free surface and interface were recorded.

When the discharge was increased, the interface rose to a higher position and the cone in the vicinity of the well

became steeper. In the later stages, as the critical condition was approached, only a slight increase in production rate would raise the cone near the well by a significant amount. The experiment was continued until the cone became almost vertical near the well. Any further increases in the production rate forced the cone to become unstable and eventually the well produced water along with oil. Just before this happened, the cone was considered as "critical." The discharge without producing water corresponding to this critical condition was measured. This completed the set of observations that were needed to analyze the performance of a partially penetrating well for a given set of aquifer conditions and well geometry. Similar experiments were made with several other sets of prototype conditions.

Summary of Experimental Results

As mentioned previously, a major purpose of the laboratory experiments was to assess the validity of existing theories relative to upconing beneath pumping wells. The theories of Wang (1965) and Muskat and Wyckoff (1935) were of particular interest. Wang assumed that the steady flow of water in the fresh water layer could be approximated mathematically by flow to a partially penetrating well pumping from a confined aquifer of thickness equal to the undisturbed thickness of the fresh water layer. This assumption permitted the calculation of the drawdown in the pumped well. Muskat's (1965) theory of partially penetrating wells was used for this purpose. The next step was to assume that the drawdown

in the well was related to the height of interface upconing by the Ghyben-Herzberg relation presented earlier as equation 13. The result was a method for computing the height of upconing as a function of well discharge that predicted no salt water entrainment until the interface reached the bottom of the partially penetrating well. The maximum discharge for which no salt water entrainment occurs is called the critical discharge. In the case of the Wang theory, the critical discharge is that which will cause the interface to rise to the bottom of the well.

The Muskat and Wyckoff (1935) theory also made use of the potential distribution calculated for a partially penetrating well in confined aquifer. Unlike the Wang theory, however, the Muskat-Wyckoff procedure used the vertical distribution of hydraulic head beneath the well to locate the highest stable interface position. The highly restrictive Ghyben-Herzberg equation was not used, and, therefore, resulted in a more physically sound relationship between the well discharge and interface upconing. The critical discharge occurs before the interface has risen to the bottom of the well in this case.

The experimental results were obtained as explained in earlier sections. In Tables 1 through 3, $\hat{D}$, Q, and $\hat{C}$ denote respectively the critical drawdown, discharge and the amount of coning below the well. The suffixes E, W, and M designate the corresponding values obtained by using experimental data, Wang's approach, and Muskat's procedure, respectively.

Table 1. Experimental Results

Case #	α	γ	$\hat{D}_E$ cm	Q_E cc/sec	$\hat{C}_E$ cm	coning (%)
1	0.743	0.0956	1.60	7.50	6.10	95.31
2	0.635	0.0956	2.50	10.60	8.45	94.13
3	0.568	0.0956	3.15	11.50	9.74	90.48
4	0.450	0.0956	4.35	12.30	11.30	82.48
5	0.541	0.0933	4.60	11.50	9.90	84.61
6	0.660	0.0915	3.20	9.30	7.50	88.24

α = fraction of fresh water thickness penetrated by well
γ = slimness ratio = radius of well divided by fresh-water thickness

Table 2. Results from Wang's Theory

Case #	α	γ	$\hat{D}_W$ cm	Q_W cc/sec	$\hat{C}_W$ cm	coning (%)	Error in Q_W (%)
1	0.743	0.0956	2.067	10.592	6.40	100.00	41.23
2	0.635	0.0956	2.938	15.982	9.10	100.00	50.77
3	0.568	0.0956	3.407	18.968	10.80	100.00	64.94
4	0.450	0.0956	4.424	22.842	13.70	100.00	85.71
5	0.541	0.0933	3.778	16.123	11.70	100.00	40.20
6	0.660	2.869	2.869	11.937	8.84	100.00	28.36

Table 3. Results from Muskat's Theory

Case #	α	γ	$\hat{D}_M$ cm	Q_M cc/sec	$\hat{C}_M$ cm	Coning (%)	Error in Q_M (%)
1	0.743	0.0956	2.309	8.653	5.35	83.59	15.37
2	0.635	0.0956	3.802	12.752	7.60	83.46	20.30
3	0.568	0.0956	4.617	14.007	8.84	81.84	21.80
4	0.450	0.0956	5.465	15.863	10.71	68.20	28.97
5	0.541	0.0933	4.394	13.069	9.31	79.56	13.64
6	0.660	0.0915	3.232	11.564	7.15	83.32	24.34

Figure 3 shows a comparison of the critical discharge obtained by the three methods. The comparison indicates the following points:

1. Wang's theory always overestimates the critical discharge. This departure from the experimental results is more conspicuous at smaller values of α than at larger values. Wang's theory, however, can be expected to predict a reasonable value of critical discharge at very large values of α. This can be explained as follows. Production from a well with a shallower penetration results in a steeper critical cone. When the brine cone is not too steep, the vertical flow components near the well are relatively less significant. In such a case, the Ghyben-Herzberg relation,

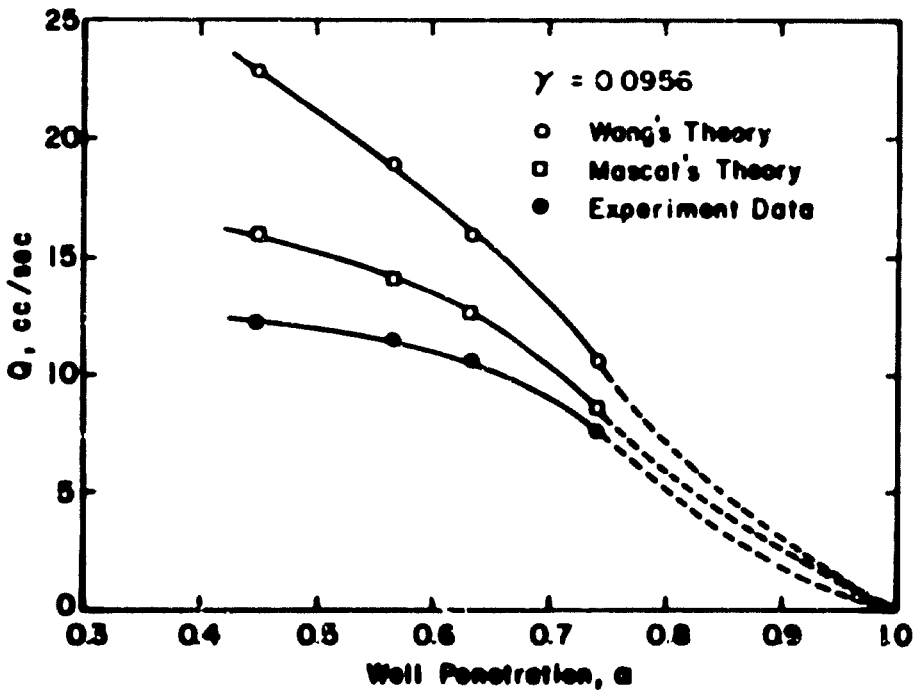

Figure 3. Comparison of theoretical critical discharge with the experimental results.

which is the basis of Wang's theory, is not too serious an approximation. Therefore, the critical discharge computed by using Wang's skimming well formula shows relatively better agreement with the experimental values for wells with deeper penetration. On the other hand, in a case of shallow-well penetration, the cone beneath the well is relatively steep. The vertical flow components, especially in the immediate vicinity of the well, cannot be neglected in this case and the Ghyben-Herzberg approximation is no longer valid. The resistance to flow due to much stronger convergence toward the well affects the potential field in the flow region. This explains why a more conspicuous departure of Wang's predictions from the experimental results occurs at relatively smaller values of α.

Further, it would seem possible to explain why Wang's theory always overestimates the critical discharge regardless of the value of α by the fact that Wang's analysis assumes that a stable brine cone could reach the bottom the well for a certain drawdown, called the critical drawdown, and remain there in static equilibrium. With this assumption, the critical drawdown is computed from the Ghyben-Herzberg relation as that drawdown for which the coning below the well is equal to the height of the bottom of the well above the original position of the interface. This value of drawdown is in turn used to calculate the critical discharge. Experiments have shown beyond doubt that, in fact, the cone does become unstable before it can rise to the bottom of the

well. Therefore, one would expect that the value of the critical drawdown used in Wang's analysis should always be greater than the actual critical drawdown which in turn results in an overestimation of critical discharge by Wang's formula.

2. Muskat's analysis of the coning problem is also only an approximate one. The potential distribution in this technique is obtained from the formulas which assume that the lower boundary of the flow region is horizontal and remains fixed. Thus the perturbation in the potential field due to the rise of the interface is not taken into account. Further, these formulas also assume a uniform flux density at all points on the surface of a well partially penetrating into the aquifer. This is not true in the rigorous sense. However, Muskat's analysis does consider the important physical phenomenon of the instability of the rising cone beneath the well. Table 3 shows that the height of the critical cone, that is, the highest stable cone beneath the well, as computed by Muskat's method, is always less than the height of the bottom of the well. Also, the critical discharge calculated by this method is in much better agreement with the experimental values than are the results obtained from Wang's formula as illustrated by Figure 3.

Thus, both methods of analysis of the coning problem, namely those given by Wang and Muskat, are only approximate ones and both have their own limitations. Nevertheless, the results show that Muskat's analysis is more realistic than Wang's analysis.

MATHEMATICAL MODELS

Several mathematical models of flow in fresh-saline water aquifers were developed as part of this study. The models fall into two broad categories: analytical models and numerical models. Each model was developed for a specific purpose and was built upon its predecessor. The function of the analytical models is to provide a relatively simple means for making design calculations while the more realistic numerical models were used to determine the effects of parameters and conditions that could not be included in the analytical models.

Interface Upconing Beneath a Horizontal Drain

The situation to be considered is depicted in Figure 4. Flow occurs toward a drain of radius a, the center line of which is a distance D below the original water table. A constant-head boundary is located a distance L from the drain. In practical cases $D << d$ and the contribution to the drain discharge due to flow above the elevation of the drain is small compared to that from below the drain. Therefore the problem can be idealized as shown in Figure 5.

Subject to the boundary conditions that $H = m$ at $x = L$ and that $H = d$ on $x^2 + z^2 = a^2$, the drain discharge is approximated by

$$Q = -\frac{2\pi K_f (m-d)}{\ln\left(\dfrac{\cosh \frac{\pi a}{m} - 1}{\cosh \frac{\pi L}{m} - 1}\right)} \tag{16}$$

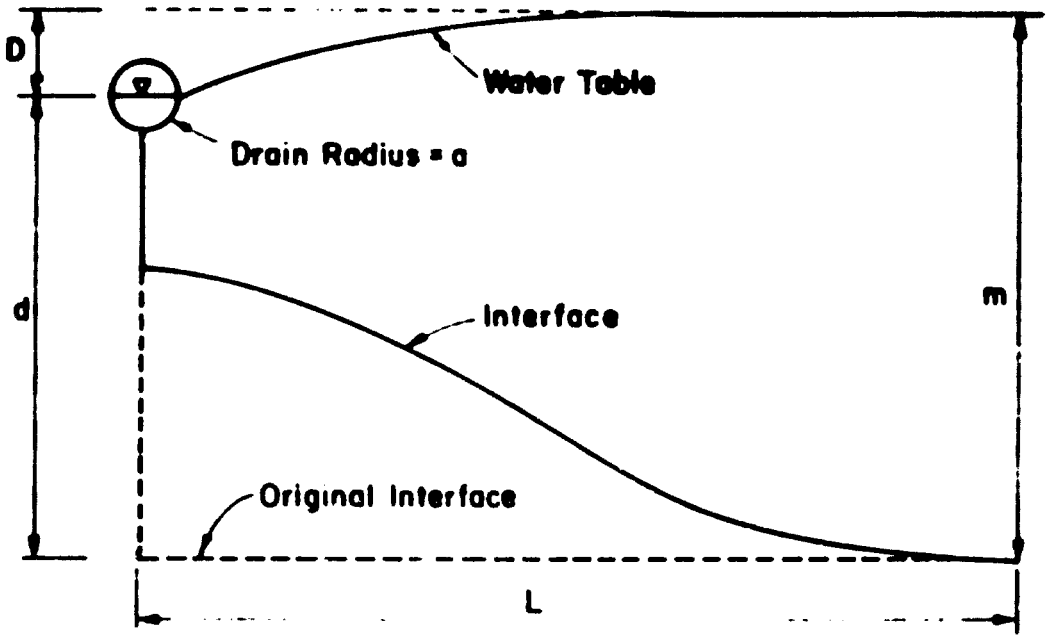

Figure 4. Flow toward a drain.

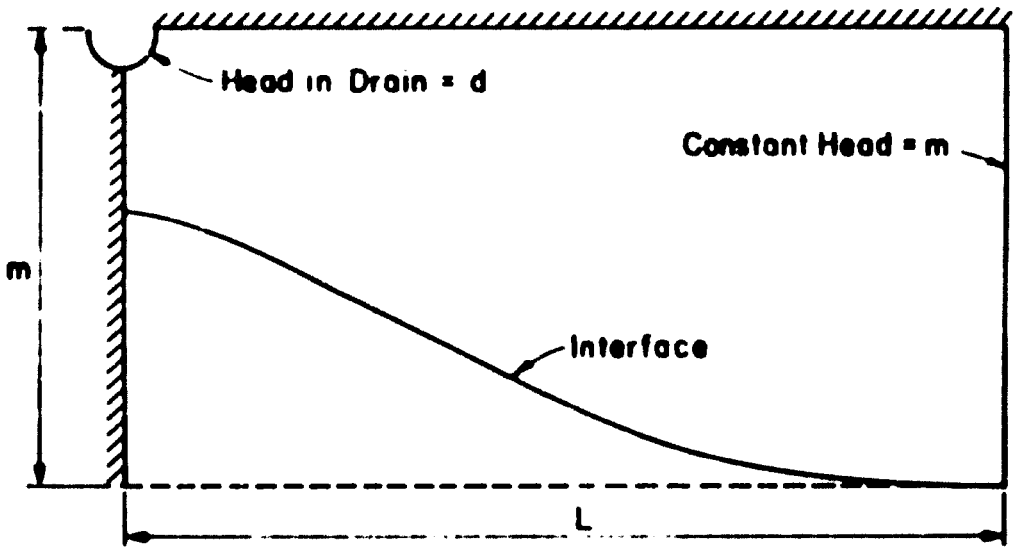

Figure 5. Idealized flow toward a drain.

and the head distribution by

$$H_f = \frac{Q}{2\pi K_f} \ln \left\{ \frac{\cosh \frac{\pi x}{m} - \cos \frac{\pi z}{m}}{\cosh \frac{\pi L}{m} - 1} \right\} + m \qquad (17)$$

Equations 16 and 17 are used to calculate the position of the interface beneath the drain in a manner similar to that used by Muskat and Wyckoff (1935) for upconing beneath a well. In the case of a pumping well, the aquifer discharge is managed by controlling the pumping rate. In contrast, the discharge from the drain will be controlled by the depth the drain is placed below the water table (i.e. by m-d). Therefore, the purpose of the analysis in the case of the drain is to determine the maximum depth below the water table that the drain can be placed without salt water entrainment.

From equation 7, the position of the interface is given by

$$\xi = \frac{\gamma_f}{\Delta\gamma} (m - H_f^{\,i}) \quad . \qquad (18)$$

According to the assumption that the upconing interface does not effect the distribution of head, the head on the interface is obtained from equation 17 with $z = m - \xi$. That is

$$H_f^{\,i} = \frac{Q}{2\pi K_f} \ln \left\{ \frac{\cosh \frac{\pi x}{m} - \cos\pi \left(1 - \frac{\xi}{m}\right)}{\cosh \frac{\pi L}{m} - 1} \right\} + m \quad . \qquad (19)$$

The simultaneous solution of equations 18 and 19 yields the unknowns $H_f^{\,i}$ and ξ at particular values of x. For design purposes the maximum elevation of the interface is of primary interest. The maximum elevation occurs directly beneath the drain on the line $x = 0$. It is convenient to

substitute equation 16 for Q in equation 19 with $x = 0$ and rearrange; this results in

$$\frac{H_f^{\,i} - d}{m - d} = 1 - \frac{\ln\left\{\dfrac{1 - \cos\pi\,(1 - \xi/m)}{\cosh \pi\, L/m - 1}\right\}}{\ln\left\{\dfrac{\cosh \pi\, a/m - 1}{\cosh \pi\, L/m - 1}\right\}} \tag{20}$$

Equation 18 is also more convenient in the form

$$\frac{H_f^{\,i} - d}{m - d} = 1 - \left(\frac{m}{m - d}\right) \frac{\Delta\gamma}{\gamma_f}\, \xi/m \tag{21}$$

Both equations 20 and 21 are dimensionless, but nevertheless a degree of generality can be gained by scaling all parameters and variables with the radius of the drain. The following scaled variables and parameters are defined:

$$\begin{aligned} \hat{H}_f &= H_f^{\,i}/a \\ \hat{d} &= d/a \\ \hat{m} &= m/a \\ \hat{L} &= L/a \\ \hat{\xi} &= \xi/a \end{aligned} \tag{22}$$

Using the above scaled variables the final form of the equations to be used in computations become

$$\frac{\hat{H}_f - \hat{d}}{\hat{m} - \hat{d}} = 1 - \frac{\ln\left\{\dfrac{1 - \cos\pi\,(1 - \hat{\xi}/\hat{m})}{\cosh \pi\, \hat{L}/\hat{m} - 1}\right\}}{\ln\left\{\dfrac{\cosh \pi/\hat{m} - 1}{\cosh \pi\, L/m - 1}\right\}} \tag{23}$$

$$\frac{\hat{H}_f - \hat{d}}{\hat{m} - \hat{d}} = 1 - \left(\frac{\hat{m}}{m - d}\right) \frac{\Delta\gamma}{\gamma_f}\, \hat{\xi}/\hat{m} \tag{24}$$

and

$$\frac{Q\,\gamma_f}{K_f m \Delta\gamma} = \frac{-2\pi\left(\frac{\hat{m}-\hat{d}}{\hat{m}}\right)\frac{\gamma_f}{\Delta\gamma}}{\ln\left\{\frac{\cosh \pi/\hat{m} - 1}{\cosh \pi\,\hat{L}/\hat{m} - 1}\right\}} \tag{25}$$

When the installation of a drain for the purpose of skimming fresh water is contemplated, the major questions are 1) how deep should the drain be located and 2) what should be the drain radius and length to achieve a certain desired discharge? Equations 23 through 25 can be used to answer these questions, at least approximately, as follows. From the field investigation the values of γ_f, $\Delta\gamma$, L , m , and K_f are measured or estimated. The radius of the largest practical circular drain is selected to determine a. Next, the values of the scaled variables $\hat{m}$ and $\hat{L}$ are computed. Using the values of $\hat{m}$ and $\hat{L}$, values of $(\hat{H}_f - \hat{d})/(\hat{m} - \hat{d})$ are calculated for several values of $\hat{\xi}/\hat{m}$ in the range $0.1 < \hat{\xi}/\hat{m} < .95$ from equation 23. A plot of the data so generated is constructed as shown in Figure 6.

Equation 24 plots as a straight line on Figure 6; the slope, however, is not known because $\hat{d}$ is not known. Therefore, the slope is adjusted so that the line representing equation 24 is tangent to the curve representing equation 23. The absolute value of the slope of the tangent line is measured and set equal to the expression for slope in equation 24. That is

$$s = -\frac{\hat{m}}{\hat{m} - \hat{d}}\,\frac{\Delta\gamma}{\gamma_f} \tag{26}$$

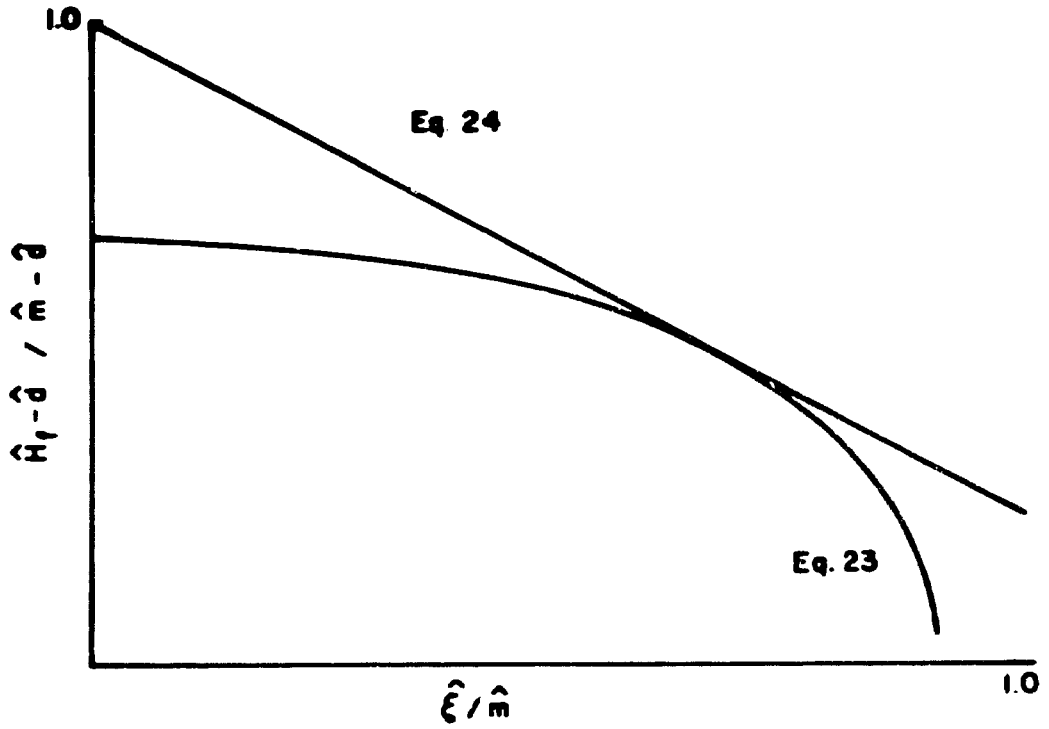

Figure 6. Graphical solution of equations 37 and 38.

where s is the slope measured from Figure 6. From equation 26, the value of $\hat{m} - \hat{d}$ is calculated. This value is the scaled depth below the original water table at which the center line of the drain should be placed.

The horizontal coordinate of the point of tangency in Figure 6 is the scaled height of the interface beneath the drain. If the straight line is drawn with a steeper slope, the point of intersection of the two curves represents a stable interface elevation at a drain depth less than the one calculated above. On the other hand, a straight line drawn so that there is no intersection represents a greater drain depth which will cause an unstable interface and salt water will be entrained. Thus the tangent condition represents the greatest safe depth at which the drain can be placed.

The next step is to use the measured value of slope and equation 25 to compute the discharge per unit length of drain. It should be pointed out that the assumptions made in the development of the above theory are such that the predicted discharge for a particular interface elevation is larger than that which would be measured. The descrepancy is probably not large for thick fresh water layers, but becomes larger for thin layers. Example calculations are provided by McWhorter (1972).

Unsteady Upconing Beneath a Pumping Well

An important practical consideration is the operating schedules of skimming wells. For example, the question of the length of time a well can be pumped at a particular rate without running a risk of pumping the underlying salt water arises. If the well is shut down, what is the rate of decline of the salt water mound is another question that might be asked. Rough answers to these questions are provided by solutions to equation 27 as demonstrated below.

McWhorter (1972) developed equation 27 following procedures introduced by Hantush (1968):

$$\frac{\partial^2 \psi}{\partial r^2} + \frac{1}{r}\frac{\partial \psi}{\partial r} = \alpha \frac{\partial \psi}{\partial t} \tag{27}$$

where $\alpha = \gamma_f S_y / \Delta\gamma K_f \sqrt{\bar{\psi}}$, $\psi = \left(\frac{m}{1-\Delta\gamma/\gamma_f} - \xi\right)^2$, and $\bar{\psi}$ is mean value of ψ. The boundary and initial conditions are

$$\lim_{r \to 0} \; r \frac{\partial \psi}{\partial r} = \frac{Q}{\pi \frac{\Delta\gamma}{\gamma_f}\left(1 + \frac{\Delta\gamma}{\gamma_f}\right) K_f} \tag{28}$$

$$\psi\,(\infty,t) = \{m/(1 + \Delta\gamma/\gamma_f)\}^2 = \psi_\infty$$

$$\psi\,(r,0) = \{m/(1 + \Delta\gamma/\gamma_f)\}^2 = \psi_o \tag{29}$$

where m is the thickness of the fresh water zone and Q is the well discharge. The solution is

$$\psi = \psi_{\infty} - \frac{Q}{2\pi\frac{\Delta\gamma}{\gamma_f}\left(1 + \frac{\Delta\gamma}{\gamma_f}\right) K_f} W(u) \tag{30}$$

where

$$W(u) = \int_{\frac{r^2 a}{4t}}^{\infty} \frac{e^{-u}}{u} du \tag{31}$$

The function W(u) is the exponential integral which is tabulated in several standard mathematical tables and all modern texts dealing with groundwater hydrology.

The above solution in ψ describes the time and spatial variation of ψ for constant well discharge. The relationship of ψ to the interface elevation ζ is given by the definition of ψ following equation 27. Values of ψ (and therefore ζ) influenced by variable pumping rates can be estimated by applying the principle of superposition.

Starting at t = 0, a well is pumped at the rate Q_1 for a time t_1 and then at Q_2 as shown below.

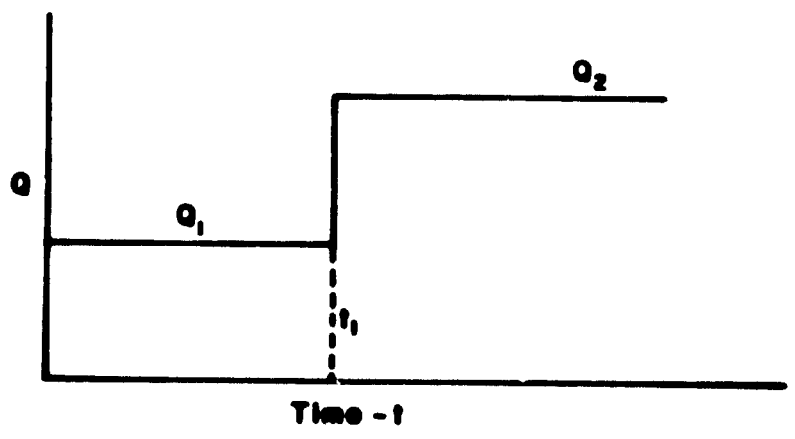

Figure 7. An example pumping schedule.

The corresponding interface elevation beneath the well is shown schematically in Figure 8.

The ordinate A at a particular time $t > t_1$ is the elevation of the interface if the pumping rate had continued at Q_1. The value of B is the additional elevation caused by increasing the rate by $Q_2 - Q_1$. The value of ψ for $t < t_1$ is calculated directly from equation 30, and ψ for $t > t_1$ is computed by extending this solution forward in time beyond t_1 and adding to it the solution for discharge at the rate $Q_2 - Q_1$ beginning at $t = t_1$. Mathematically, this statement is

$$\psi(r_w,t) = \left(\frac{m}{1 + \Delta\gamma/\gamma_f}\right)^2 - \left(\frac{Q_1}{2\pi \frac{\Delta\gamma}{\gamma_f}\left(1 + \frac{\Delta\gamma}{\gamma_f}\right) K_f} W(t)\right.$$

$$\left. + \frac{(Q_2 - Q_1)}{2\pi\frac{\Delta\gamma}{\gamma_f}\left(1 + \frac{\Delta\gamma}{\gamma_f}\right) K_f} W(t - t_1)\right) \qquad (32)$$

where $W(t)$ is the function given in equation 31 with $r = r_w$ and $W(t - t_1)$ is the same function with $r = r_w$ and t replaced by $t - t_1$.

The above process can be extended to any number of steps in discharge. The result for n steps is

$$\psi(r_w,t) = \left(\frac{m}{1 + \Delta\gamma/\gamma_f}\right) - \frac{1}{2\pi \frac{\Delta\gamma}{\gamma_f}\left(1 + \frac{\Delta\gamma}{\gamma_f}\right) K_f}$$

$$\left(Q_1 W(t) + \sum_{i=2}^{n} (Q_i - Q_{i-1}) W(t - t_{i-1})\right). \qquad (33)$$

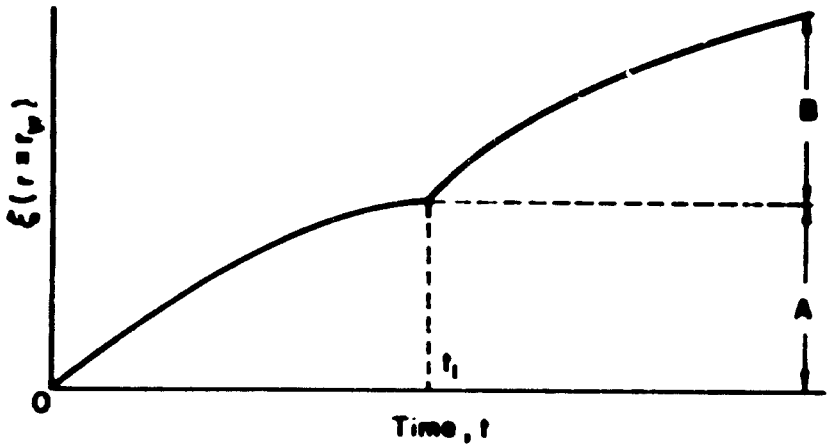

Figure 8. Schematic of the interface elevation corresponding to the pumping schedule shown in Figure 7.

In the limit as the variation of discharge becomes continuous, equation 33 becomes

$$\phi(r_w,t) = \left(\frac{m}{1 + \Delta\gamma/\gamma_f}\right) - \frac{1}{2\pi\frac{\Delta\gamma}{\gamma_f}\left(1 + \frac{\Delta\gamma}{\gamma_f}\right) K_f}$$

$$\left\{Q_1\, W(t) + \int_0^t \frac{dQ}{d\tau}\, W(t - \tau)\, d\tau\right\} \qquad (34)$$

which is the familiar convolution integral.

Equations 33 or 34 can be used to calculate the growth and decay of the salt water mound in response to any variation in pumping rate.

The principle of superposition can also be used to calculate the effects of well interference. This is an important consideration because the interface elevation in the vicinity of interferring wells is higher than one would calculate taking each well individually.

Since equation 27 is linear, the value of ϕ at any particular point in a well field can be calculated by adding the values of ϕ produced at the point by each individual well. Thus,

$$\phi_t = \sum_{i=1}^{n} \phi_i \tag{35}$$

where ϕ_i is the value of ϕ produced by the ith well and ϕ_t is the total.

An important conclusion of the unsteady analysis is that wells can be pumped at high rates for short periods of time without entraining salt water because a volume of water equal to that between the initial and the upconed interface must be pumped in order to establish a given interface position. This conclusion is not apparent in the steady flow theories where a steady position of the upconed interface is presumed at the outset.

The Effect of Anisotropy

Because a reduced vertical permeability relative to the horizontal permeability has a marked influence on the distribution of hydraulic head, it might be expected that anisotropy would modify the conclusions concerning optimum pumping rates and penetration ratios derived for isotropic aquifers. Chandler (1973) modified and improved the model of Sahni (1972) to include the effects of differing vertical and horizontal permeabilities. These results were also reported by Chandler and McWhorter (1975).

Radially symmetric, steady flow in a homogeneous and anisotropic aquifer is governed by:

$$\frac{K_r}{r}\frac{\partial}{\partial r}\left(r\frac{\partial H}{\partial r}\right) + K_z\frac{\partial^2 H}{\partial z^2} = 0 \tag{36}$$

where

H = piezometric head (L),

K_r = hydraulic conductivity in the horizontal direction (L/T),

K_z = hydraulic conductivity in the vertical direction (L/T),

r = radial coordinate measured from well axis (L),

z = vertical coordinate measured positive upward from the original interface elevation (L).

Equation 36 was written on the assumption that the principal directions of hydraulic conductivity coincide with the r and z coordinate directions.

The fresh water flow region is bounded on the top by a stationary water table; a surface on which the pressure is everywhere atmospheric. The lower boundary of the fresh water region is a stationary surface, which mathematically, constitutes an impermeable surface. These conditions and additional ones used for the solution of equation 1 are depicted in Figure 9. The requirement that the water table and the interface be stream surfaces can be shown to constitute nonlinear boundary conditions.

Solutions for the anisotropic case were obtained by solving the transformed equation

$$\frac{\partial}{\partial r_t} \left(r_t \frac{\partial H}{\partial r_t}\right) + \frac{\partial^2 H}{\partial z^2} = 0 \tag{37}$$

where

$$r_t = \left(\frac{K_z}{K_r}\right)^{1/2} r \tag{38}$$

and transforming the results back into the real (r,z) domain.

A fully implicit numerical technique was used to integrate equation 37 subject to the boundary conditions shown in Figure 9. The initial iteration was performed using a horizontal water table and a horizontal interface. From the resulting distribution of head, the position of the water table was established by determining the locus of points of atmospheric pressure. At the interface, equation 18 must be satisfied with $m = H_e$. The position of the interface following the first iteration was established by determining the locus of points in the flow region for which equation 18 is satisfied. The second iteration was performed using the water table and interface surfaces located from the previous iteration. Finite difference grids that were found to fall outside of the flow domain after each iteration were subsequently treated as no-flow grids. Iteration was continued until the maximum difference in head between successive iterations was less than some arbitrary value. Usually, only three iterations were required to obtain a stable solution.

The mathematical model was compared with the familiar steady-state solution based on the Dupuit-Forchheimer assumptions for a fully penetrating well in a homogeneous and isotropic aquifer with no upconing. Identical boundary conditions

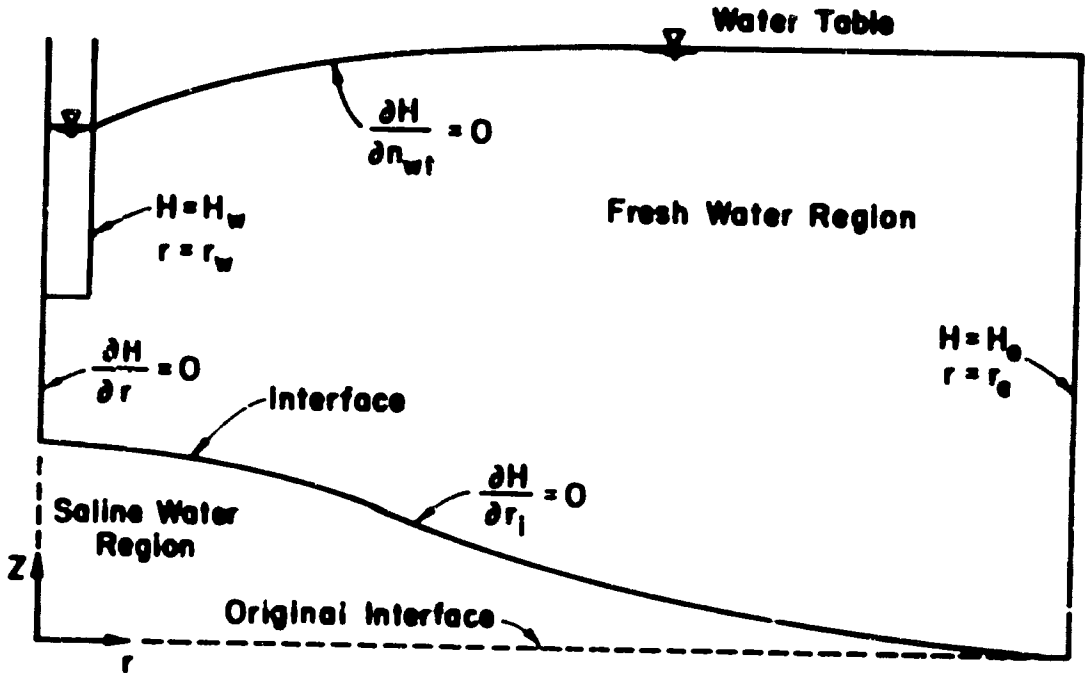

Figure 9. Definition sketch for upconing of salt water beneath a pumped well.

at $r = r_e$ and at $r = r_w$ were used in the finite difference model and the approximate analytical solution. The configuration of the water tables calculated by the two methods agreed very well. The well discharge computed from the numerical model was 1.7 percent higher than that computed from the approximate analytical solution.

A comparison with Sahni's (1972) experimental results was conducted to establish the validity of the model component concerned with upconing of the heavier liquid. A comparison of the calculated interface and water table profiles with Sahni's measured profiles is shown in Figure 10. The predicted and measured profiles agree closely. It is important, however, that the numerical model also satisfactorily predicts the critical conditions. A comparison of the measured and predicted drawdown, cone height beneath the simulated well, and the well discharge for the critical condition is presented in Table 4. The correspondence between the measured and predicted values shown in Table 1 is satisfactory, considering that Sahni's experiments were not

Table 4. Measured and Predicted Critical Conditions

	Critical Drawdown (cm)	Critical Interface Elevation (cm)	Critical Drawdown (cm^3/sec)
Measured	3.2	7.5	9.3
Predicted	3.04	8.33	10.62

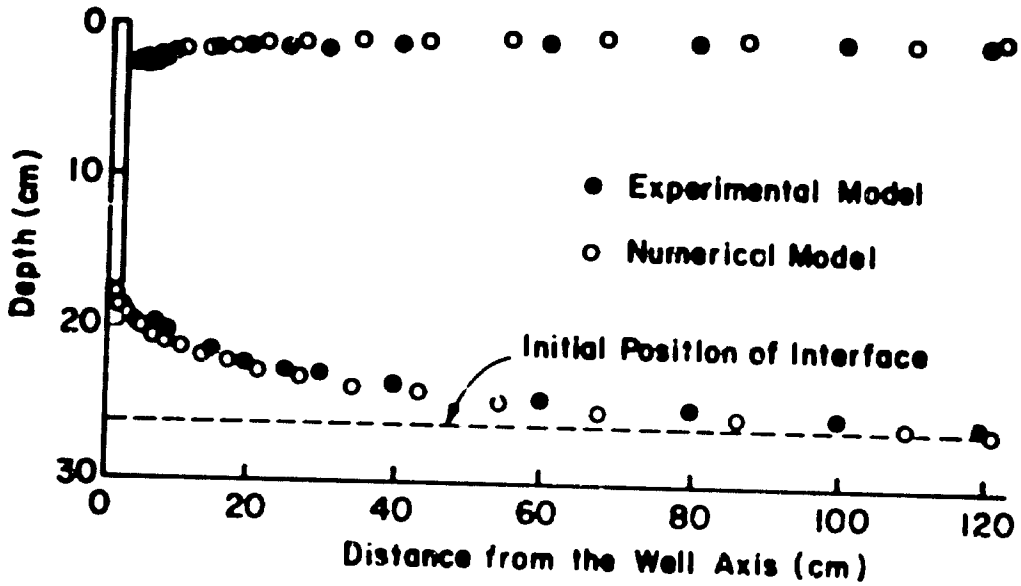

Figure 10. Comparison of measured and calculated results for flow to a well in an isotropic aquifer.

completely free of capillary effects which are not included in the numerical model and that the exact critical condition is difficult to establish experimentally.

The maximum critical pumping rate that can be maintained without causing the saline water to rise above critical elevation depends upon the fraction of the fresh water layer penetrated by the well. It is desirable to determine the degree of penetration which permits the maximum critical pumping rate. The critical discharge is shown as a function of well penetration in Figure 11 for an isotropic aquifer and for three anisotropic aquifers. The results are presented in dimensionless form for convenience and maximum generality. The definitions of the dimensionless critical discharge and well penetration are:

$$\hat{Q}_c = \frac{\rho_f Q_c}{\Delta\rho \, H_e^2 K_r} \tag{39}$$

and

$$\alpha = d_w/H_e \tag{40}$$

respectively, where Q_c is the critical well discharge, d_w is the depth of the well below the undisturbed water table, H_e is the undisturbed fresh water thickness, ρ_f = fresh water density, $\Delta\rho$ = density difference, and other symbols are as previously defined.

The critical discharge is low for all cases when the well penetration is to a point near the undisturbed interface

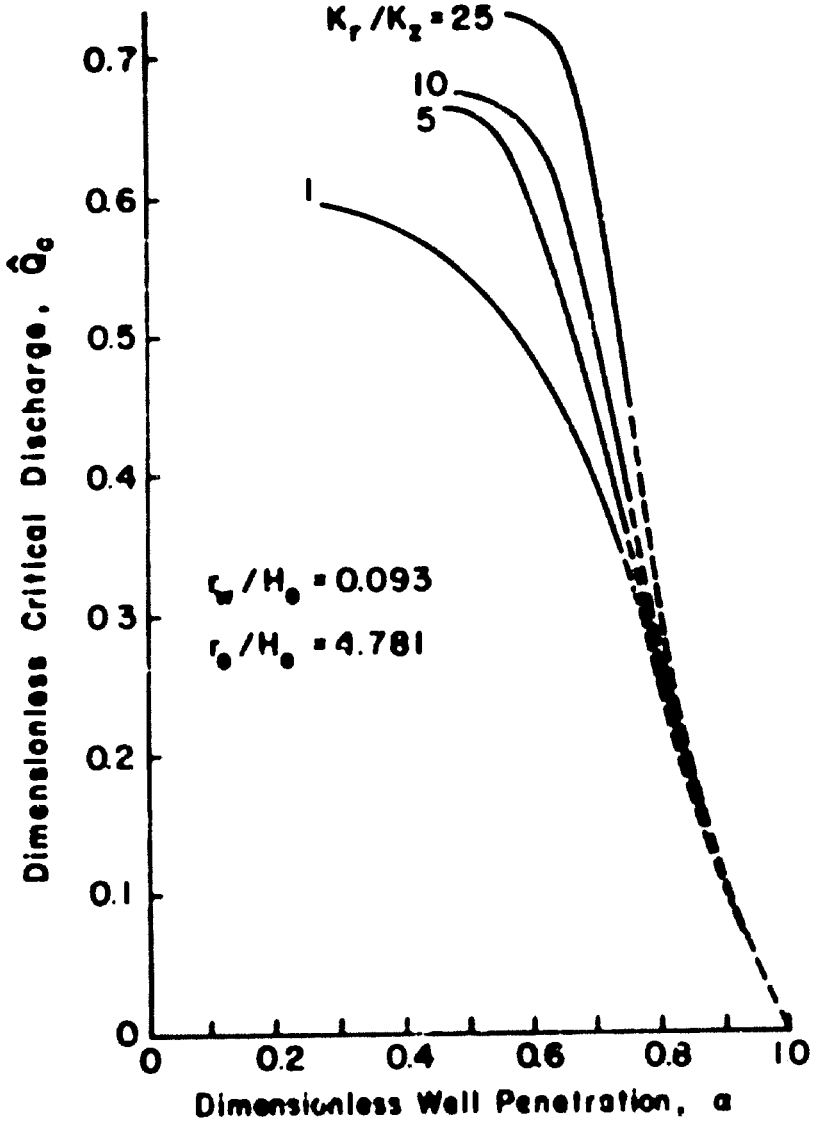

Figure 11. Critical discharge as a function of well penetration.

because the interface must rise only a short distance to reach the critical elevation. Thus, the critical elevation is produced by a small drawdown at the well with a corresponding small discharge. At very small penetrations (i.e., $0<\alpha<0.3$), the maximum permissible drawdown and discharge are limited by the well hydraulics and not by a critical interface elevation. In other words, the maximum hydraulically possible discharge is insufficient to produce a critical upconing condition. The end points of the four curves indicate the maximum critical discharge obtainable in each case.

The end points of the curves in Figure 11 show that the optimum penetration increases with increasing ratios of horizontal to vertical permeability. The relationship between optimum penetration and permeability ratio is shown explicitly in Figure 12. Wang (1965) also predicted that the optimum penetration increases with increasing ratios of horizontal to vertical permeability. The optimal penetration predicted herein is somewhat greater than predicted by Wang, however.

The elevation of the interface beneath the well increases as the well discharge is increased as shown in Figure 13. The dimensionless interface elevation, $\hat{\zeta}$, is defined by

$$\hat{\zeta} = \frac{\rho_f}{\Delta\rho}\frac{\zeta}{H_e} \tag{41}$$

The end points of the curves in Figure 13 represent the critical discharge and interface elevation. Of particular interest is the observation that the discharge is greater for the anisotropic than for the isotropic aquifers with the same interface

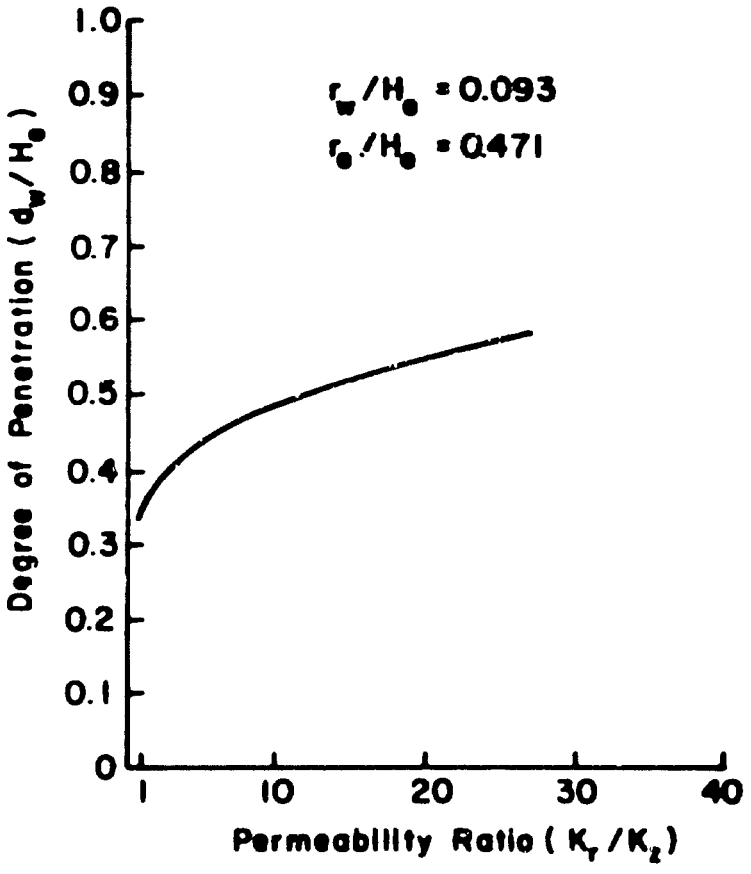

Figure 12. Relationship between optimum penetration ratio and permeability ratio.

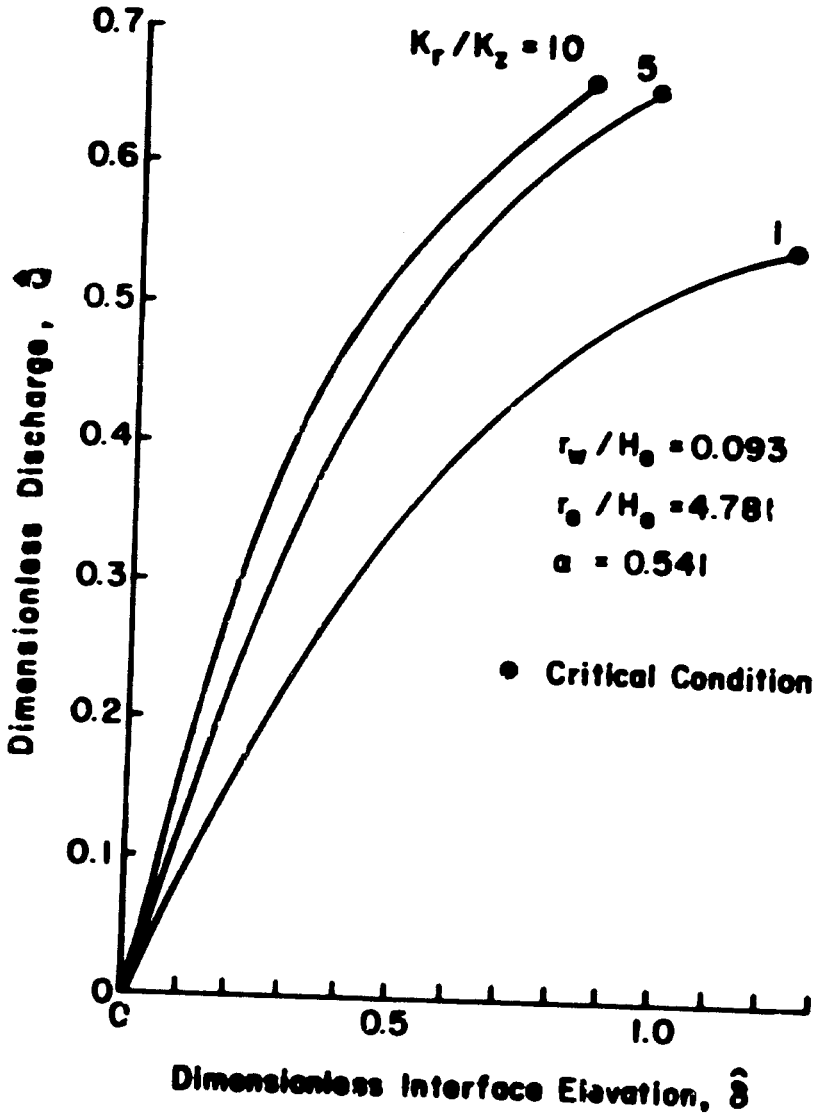

Figure 13. Relation between discharge and interface elevation for various permeability ratios.

elevation. Furthermore, the critical discharge is greater for the anisotropic case than for the isotropic case. This conclusion is in contrast to the results of Wang (1965) which indicate a smaller critical discharge for the anisotropic aquifers; other parameters remaining equal.

Anisotropy influences the hydraulic behavior in two ways which, in turn, affects the critical interface elevation and the corresponding critical discharge. Decreasing the vertical permeability, while maintaining the horizontal permeability constant, results in an overall increased resistance to flow toward partially penetrating wells which produces a greater drawdown per unit of discharge for the anisotropic aquifer. Wang (1965) assumed the interface elevation to be directly proportional to the drawdown; therefore, for equal interface elevations, the well discharge for the anisotropic case is less than for the isotropic case. Examination of equation 18 shows that Wang's assumption is tantamount to assuming that the head H^i on the interface beneath the well is equal to the head in the well. Such a situation is possible only if there exist no vertical components of flow.

The second effect (which was neglected by Wang) of a reduced vertical permeability is to increase the total head loss along a vertical line beneath the well as compared to the isotropic case with the same drawdown in the well. In other words, the head, at any point beneath the well, is greater for the anisotropic than for the isotropic case; all

other parameters being equal. It is clear from equation 18 that the elevation of the interface is, therefore, depressed by the effects of anisotropy. This fact permits the maximum safe drawdown to be significantly greater for wells pumping from anisotropic aquifers. Evidently, the increase in the maximum drawdown allowable in the anisotropic aquifer is sufficient to more than offset the effects of increased resistance to flow, resulting in a higher allowable well discharge.

The analyses of Wang (1965) and Muskat and Wyckoff (1935) linearize the boundary condition on the interface by ignoring the influence of the interface upconing on the distribution of head in the fresh-water zone. The effect of the upconing is to cause additional convergence of flow and a corresponding decrease in discharge per unit of drawdown. The critical discharge predicted by neglecting the upconing should exceed the actual critical discharge, therefore. Comparisons with the critical discharge predicted by the numerical model for one case indeed indicated that Wang's critical discharge was 13 percent too high. A rather extensive comparison of the results of Wang and Muskat and Wyckoff with Sahni's (1972) experimental results shows predicted critical discharges ranging up to 86 percent higher than the measured value.

The results of the analyses of upconing in anisotropic aquifers are summarized as follows. There exists an optimum degree of well penetration into the fresh water layer which permits maximum discharge without causing the heavier, saline water to rise into the well. The optimum penetration for isotropic aquifers is near 30 percent and increases to more

than 50 percent for aquifers in which the vertical permeability is less than 5 percent of the horizontal permeability. Well discharges for penetrations less than optimum are limited by well hydraulics, and for penetrations greater than optimum, by the incipient entrainment of saline water from below. The highest stable interface elevation is always less than the elevation of the bottom of the well screen.

A reduced vertical permeability results in a smaller discharge per unit of drawdown, but also permits a larger drawdown to be maintained without salt water entrainment. The latter influence is dominant, and the critical discharge for aquifers with a reduced vertical permeability is larger than for an isotropic case, other factors remaining equal. Accurate predictions of the critical well discharge cannot be made by ignoring the influence of the interface upconing on the head distribution in the fresh-water zone. Operation of a well at the critical discharge predicted by neglecting the increased convergence caused by upconing will result in salt water entrainment.

FIELD EXPERIENCES WITH SKIMMING WELLS

A set of field experiments were designed and carried out in Pakistan. One of the purposes of the field tests was to determine if the fresh-saline water system responded to pumping in a manner consistent with the laboratory and theoretical predictions. Another purpose was to determine and develop solutions to any practical problems involved in skimming well construction and use.

The site for the experiments was Phularwan Research Farm, a part of the Mona Reclamation area. This site was selected because preliminary investigations indicated a shallow water table and a zone of relatively fresh water about 100 ft thick above a much more saline body of ground water. The research plan called for testing a tubewell constructed similar to the usual private tubewell and a dug well of large diameter. Meaningful results were not obtained from the dug well experiments, and this report summarizes the results from the tubewell experiments, only. Two tubewells were eventually constructed and tested and are referred to as tubewells 1 and 2 throughout the remainder of this report.

The layout of tubewell 1 and the associated observation wells are shown in Figure 14. The initial vertical distribution of salinity, as indicated by electrical conductivity, is shown in Figure 15. The interface was taken as the depth at which the EC was equal to 5 mmhos/cm and all future references to the interface in this report correspond to an EC of 5 mmhos/cm. On this basis, the fresh water layer was determined to be about 80 ft. thick. The aquifer material is an uncemented, medium sand for which the 50% size is 0.25 mm.

The important features of the tubewell and observation wells are as follows. The tubewell penetrated to a depth of 37 ft. below the datum elevation established near the ground surface. At the time of construction, this depth represented approximately 28 ft of penetration of the fresh water zone.

Observation Well	Distance From Center of Tubewell (ft)	Top Elevation With Respect to Bench Mark (ft)
T1-1	10.6	1.48
T1-2	19.1	1.55
T1-3	38.5	1.76
T1-4	77.9	1.76
T2-1	8.9	1.64
T2-2	18.8	1.67
T2-3	39.0	1.54
T2-4	78.0	1.52

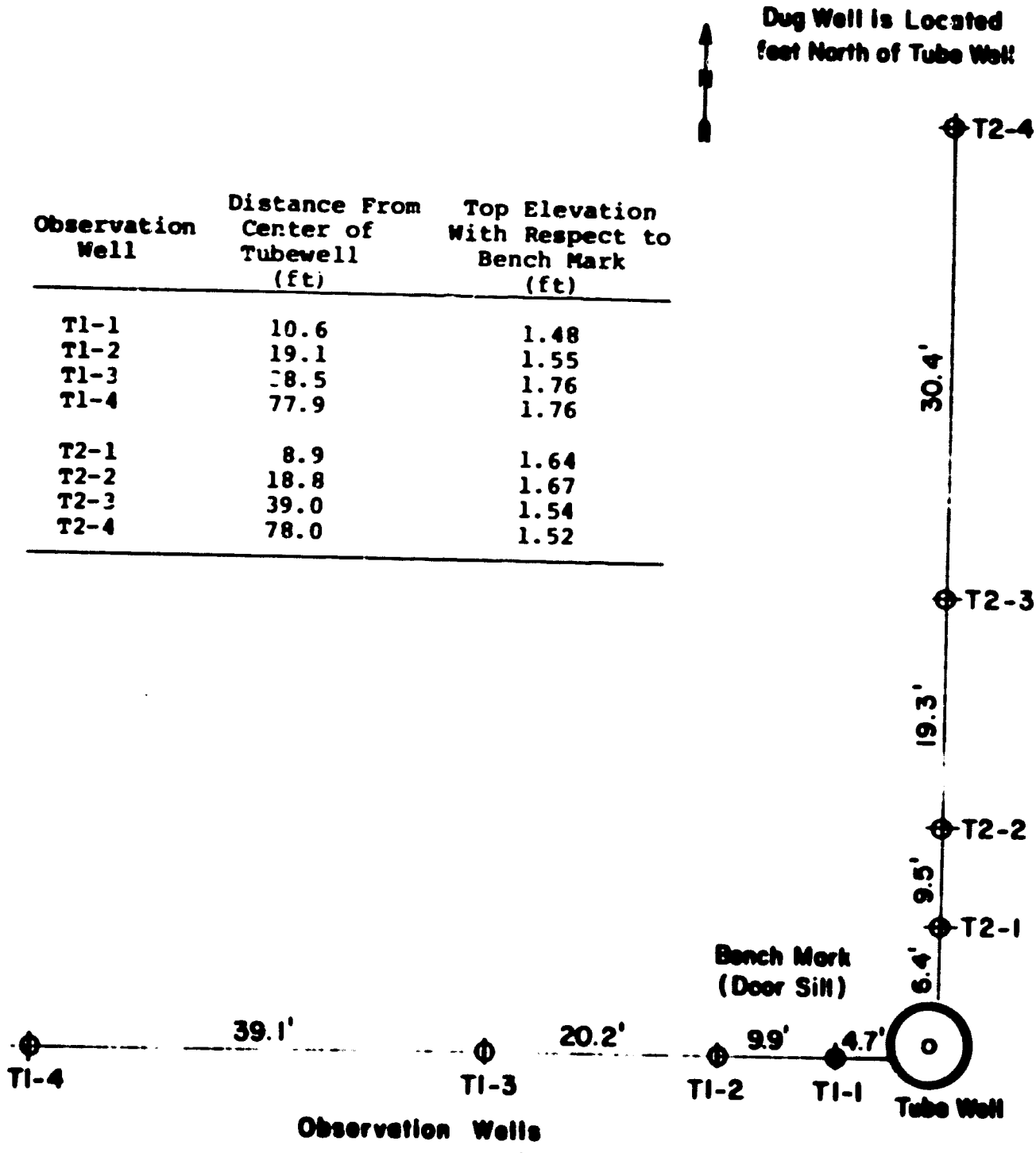

Figure 14. Tubewell and observation well layout.

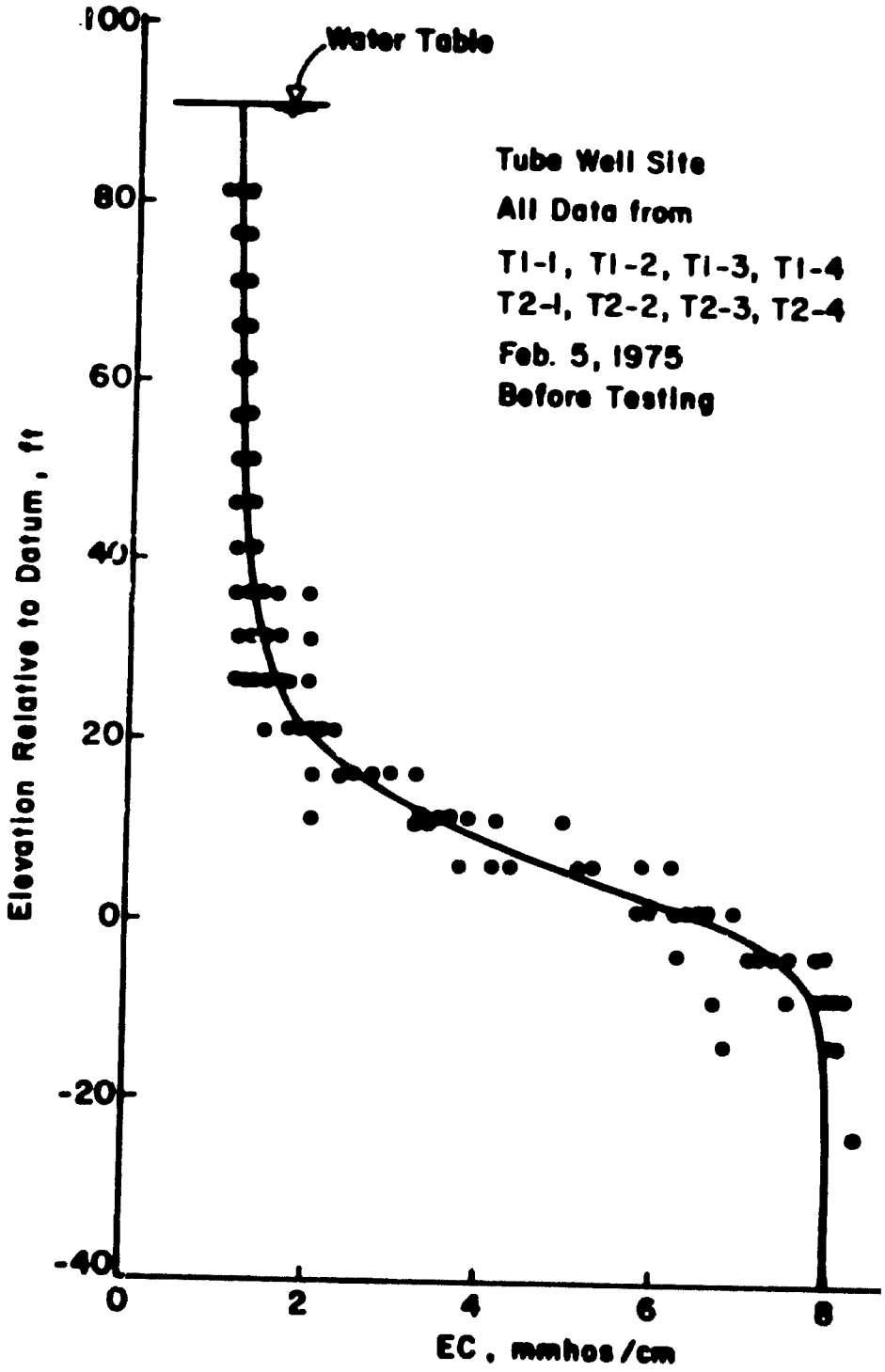

Figure 15. Salinity profile at skimming well test site.

Twenty-four feet of slotted PVC well screen extended from just below the water table to the bottom of the well. Thus, the penetration ratio was 0.3 in accordance with the theoretical optimum value. A gravel pack was placed around the screen. A locally manufactured, suction lift pump was used to lift the water during the test. The discharge was controlled with a gate valve in the discharge line and was measured using a piezometer and orifice plate. The details of the tubewell construction are shown in Figure 16.

Figure 17 shows the design and construction details of the observation wells. Use of the polypropylene tubing in a backfilled hole was a feature that resulted from initial failures of attempts to use an open hole in which the EC could be measured. The open hole observation wells failed because even the small vertical component of hydraulic gradient was sufficient to cause water to "short-circuit" from the bottom of the well to the top and to completely mask the actual vertical distribution of salinity. With the design shown in Figure 17, it was possible to obtain a sample of ground water by applying a vacuum to the piezometer tubes that terminated at 10 ft. intervals. The EC of each sample was measured to determine the distribution of salinity.

Following a set of tests with the facilities described above, a second tubewell was constructed. The screened interval in Tubewell 2 was approximately twice as long as in tubewell 1. The screen in tubewell 2 was a quire strainer (a metal frame wrapped with coconut fiber rope which is a common strainer used in private tubewells in Pakistan). The production capacity of this well was substantially greater

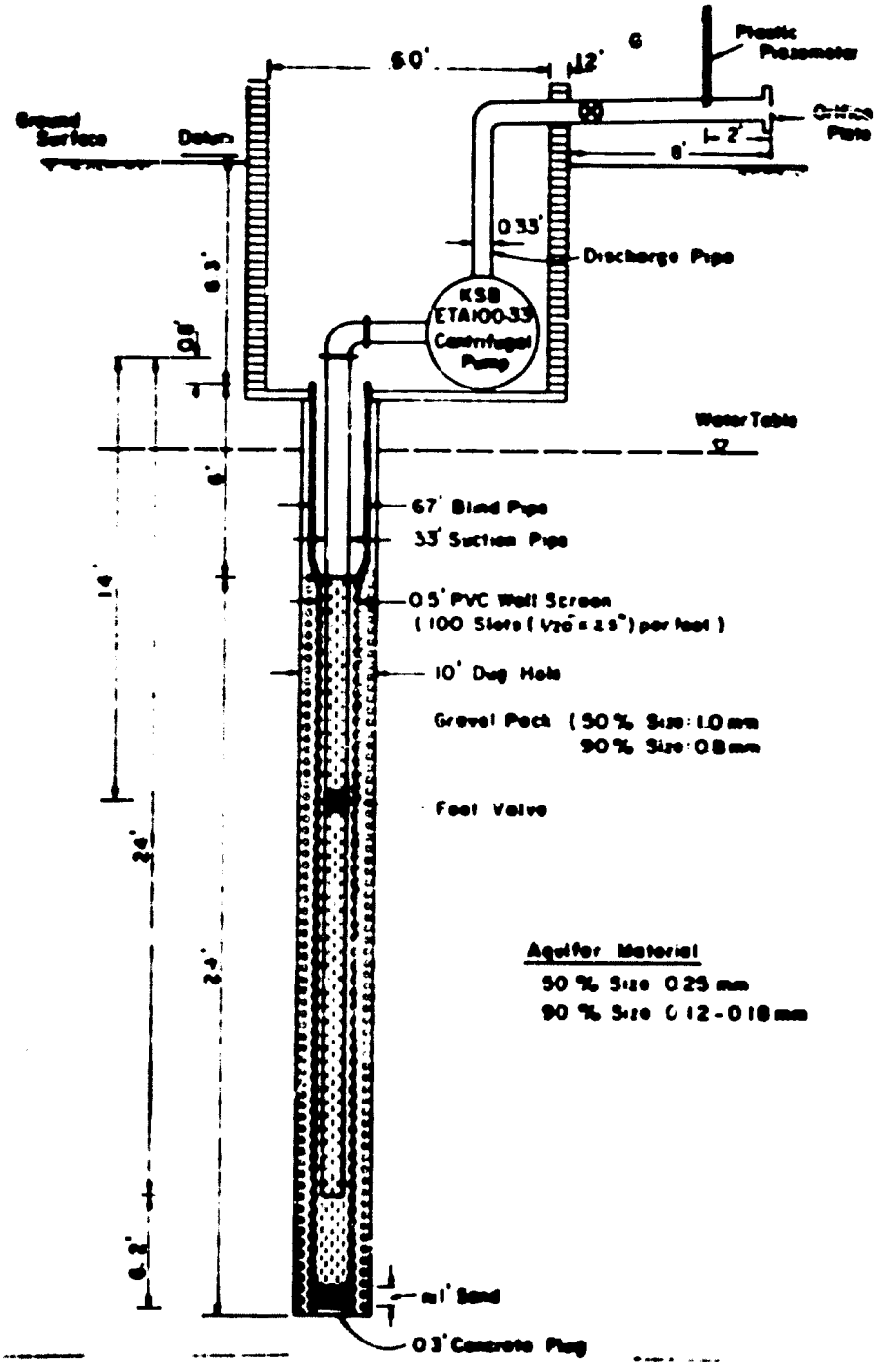

Figure 16. Tube well construction. (Not to scale.)

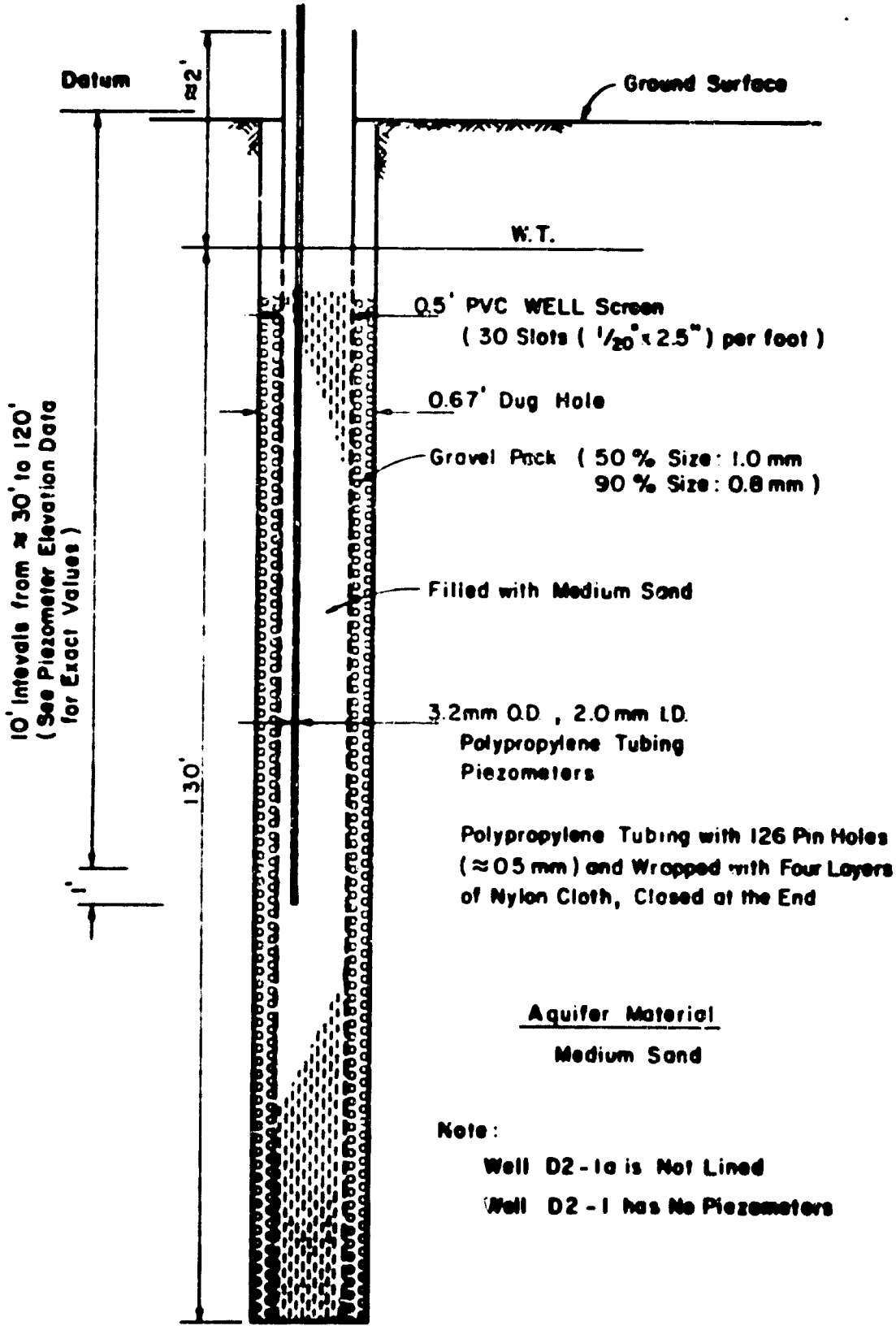

Figure 17. Observation wells--skimming well field experiment. (Not to scale.)

than for tubewell 1 and permitted the creation of a greater degree of upconing.

Summary Results

The rise of the fresh-saline water interface during a 13 day period for which the pumping rate was 65 gallons per minute (gpm) is shown in Figure 18. The data in Figure 18 are for T1-2, located 19 ft. from tubewell 1. Similar profiles were obtained at observation points located at 10, 39, and 77 ft. from the pumped well.

Tubewell 1 broke suction after 13 days of steady pumping at a rate of 65 gpm. The decline of the upconed salt water was monitored for several days following the cessation of pumping. These results are shown in Figure 19, and indicate a very slow recovery of the interface toward its initial location. During this test, a total of 1.4×10^5 ft^3 were pumped. Estimation of the volume of saline water in the upconed mound is 1.2×10^5 ft^3. This indicates that most of the pumped water was displaced by the upconing of the saline water. In order for the interface to return to its initial position, recharge into the cone of influence in the amount of 1.4×10^5 ft^3 must occur. In the absence of recharge from rain and/or deep percolation from irrigation, this quantity must be supplied by lateral inflow from areas outside the radius of influence. Lateral inflow will occur in response to residual hydraulic gradients after the cessation of pumping that are much smaller than during pumping. Therefore, it is expected that recovery of the interface will be much slower than the buildup of the cone.

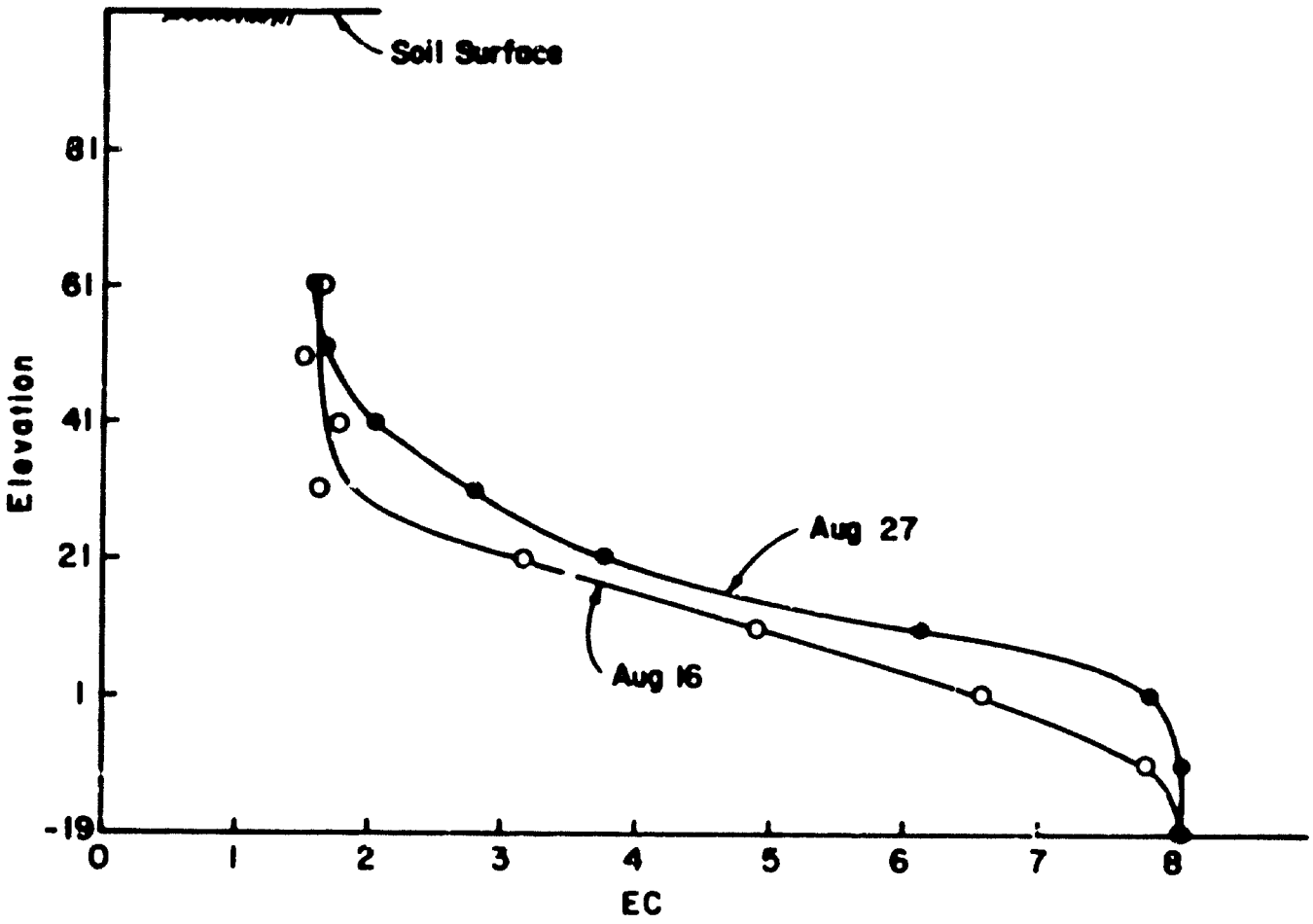

Figure 18. Salinity profile at skimming well site.

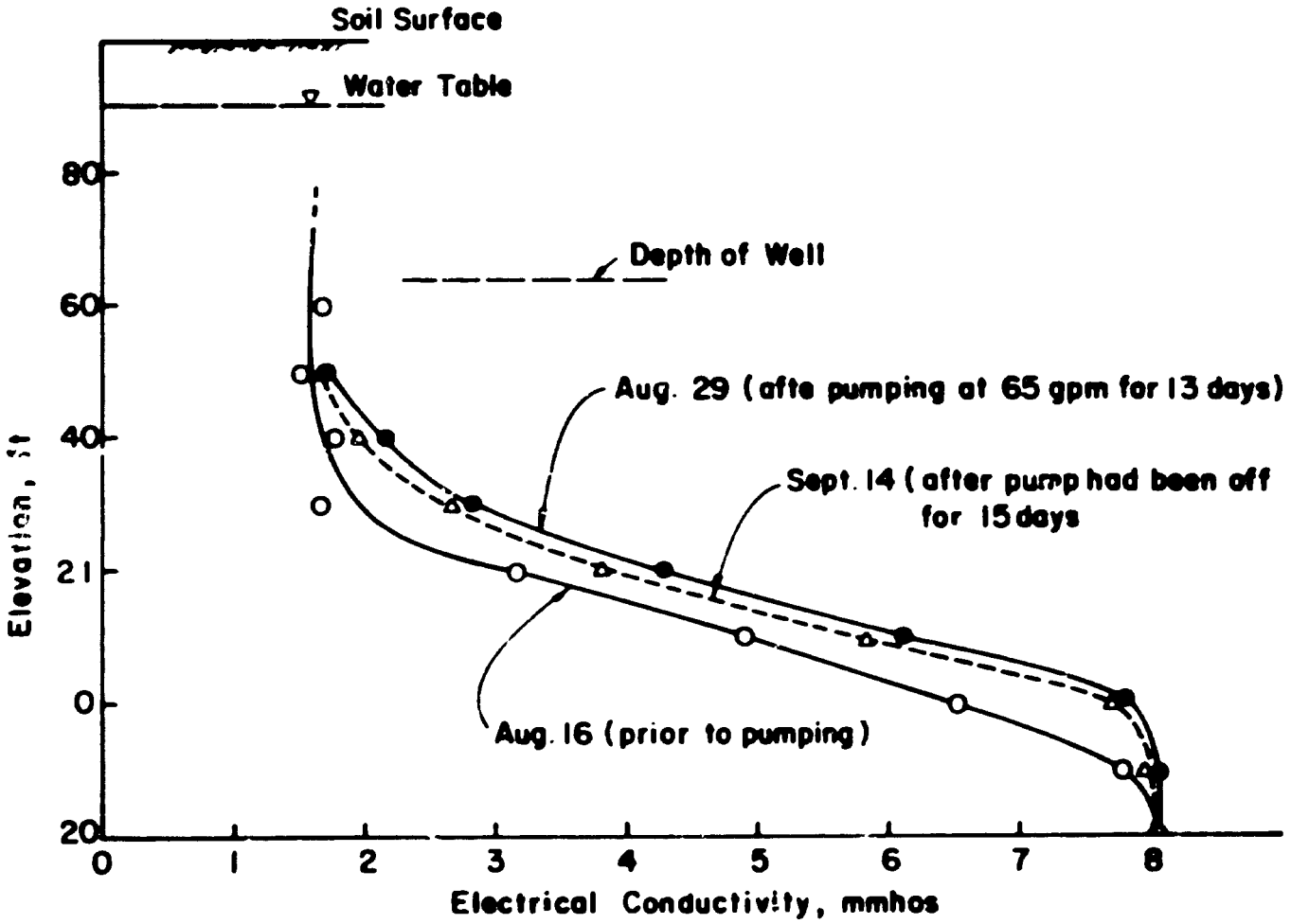

Figure 19. Observation well at T1-3.

Attempts to create a larger degree of upconing beneath tubewell 1 were not successful because of increasing severe problems with breaking suction. Head loss through the gravel pack and well screen was substantial in tubewell 1 and seemed to increase with time. Therefore, tubewell 2 was constructed so that observations with greater upconing could be made.

Tubewell 2 functioned approximately as expected delivering a continuous flow of 225 gallons per minute with a drawdown inside the strainer as indicated in the Figure 20. There was some fluctuation during the first day or two as the pack around the strainer was developing, but the drawdown within the well was remarkably stable after January 7.

The water table levels before, during and after pumping are shown in Figure 21. The water table dropped very quickly as the well began to pump and then more slowly from January 6 to January 9 as water was being continuously pumped at a rate of about 0.5 cusec (225 gallons per minute). The area around the wells was irrigated during the afternoon of January 9 and the water table had risen 4 or 5 inches by January 10. The water table declined a couple of inches between the 10th and the 15th during which there were 2 or 3 small showers and then on the 15th there was a sizable rain in the evening and by the 16th the water table had risen about 2 inches. There was no rain or irrigation from the 16th to the 20th during which the water table declined about 7 inches. After the pump was turned off the 20th, the water table rose rapidly and by

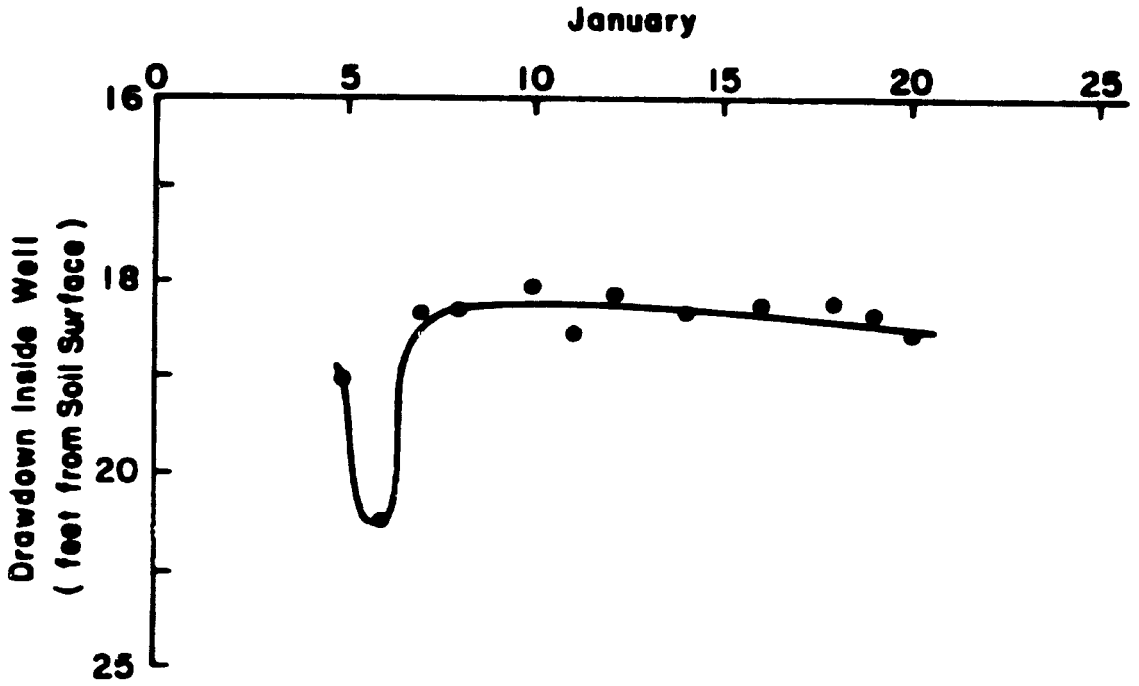

Figure 20. Level of water in tubewell 2 during pumping.

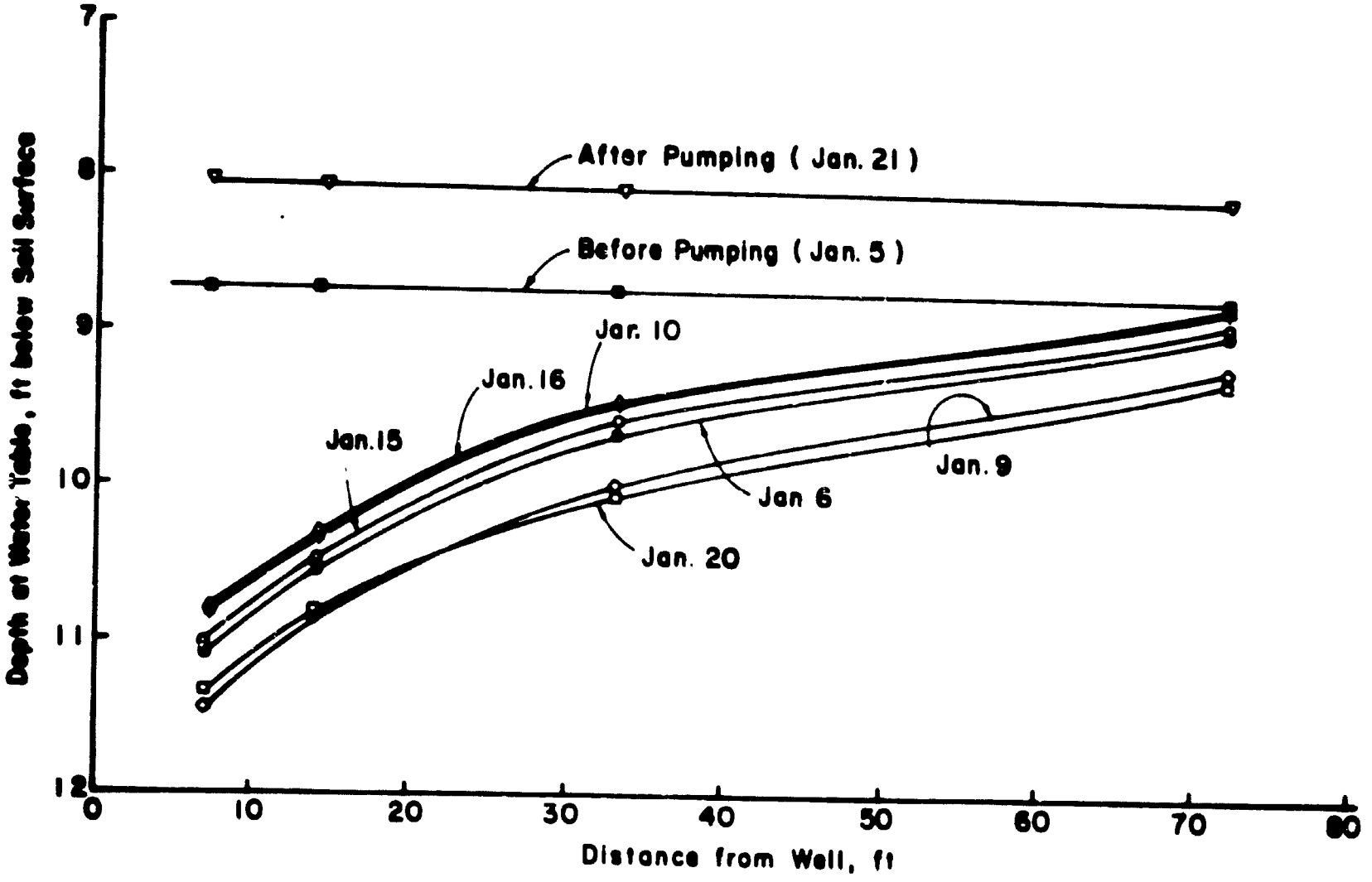

Figure 21. Water table before, after and during pumping.

the 21st was up at almost 8 feet indicating that there had been a general resupply of water to the area from the irrigation and rains received between January 5 and January 21 which was greater than the amount of water which had been pumped during that time.

The salt content as a function of depth is shown at the observation sites 8 feet, 31 feet, and 70 feet from the well, before and during pumping in Figures 22, 23, and 24, respectively. During the measurements prior to January 14 the temperature of the water was not determined when the electrical conductivity was measured. Depending upon how long the solution samples remained in the bottles after extraction and prior to measurement and the air temperature at that day, the temperatures of these samples could have ranged from 20 to 27°C. All conductivities measured on and after January 14 were accompanied by temperature measurements and are expressed in these figures as equivalent conductivities at 25°C. Consistent deviation of a few points from the curve indicates that these sampling heads are not at the specific elevation that they were supposed to have been installed. However these successive measurements show a consistent rise in a cone year the well.

Since the electrical conductivity of 5 mmhos is approximately the midpoint between the conductivity of the fresh and and saline waters, this electrical conductivity was chosen as the concentration indicating the interface between the

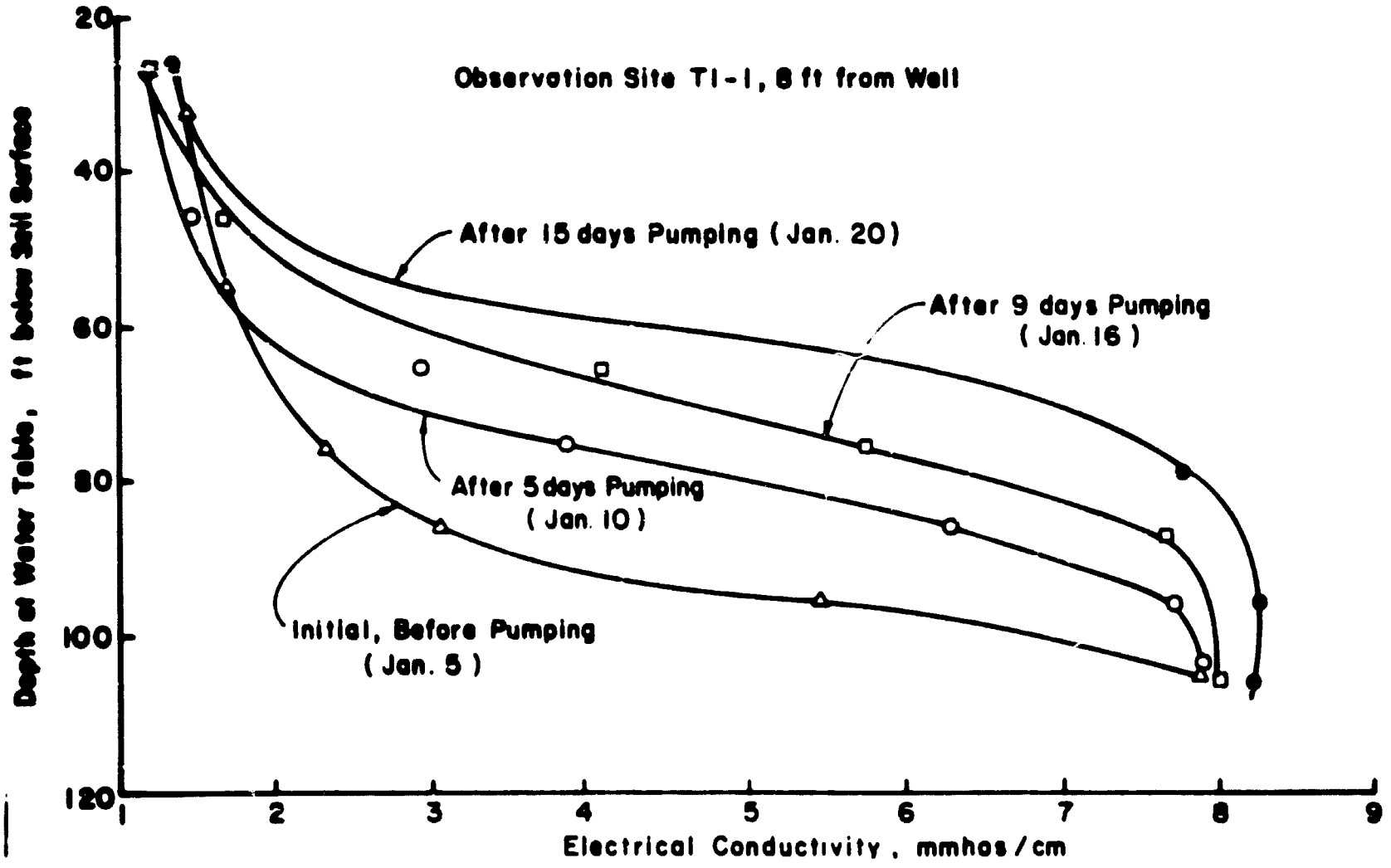

Figure 22. Salinity of water in the aquifer as a function of depth below the surface before and during pumping.

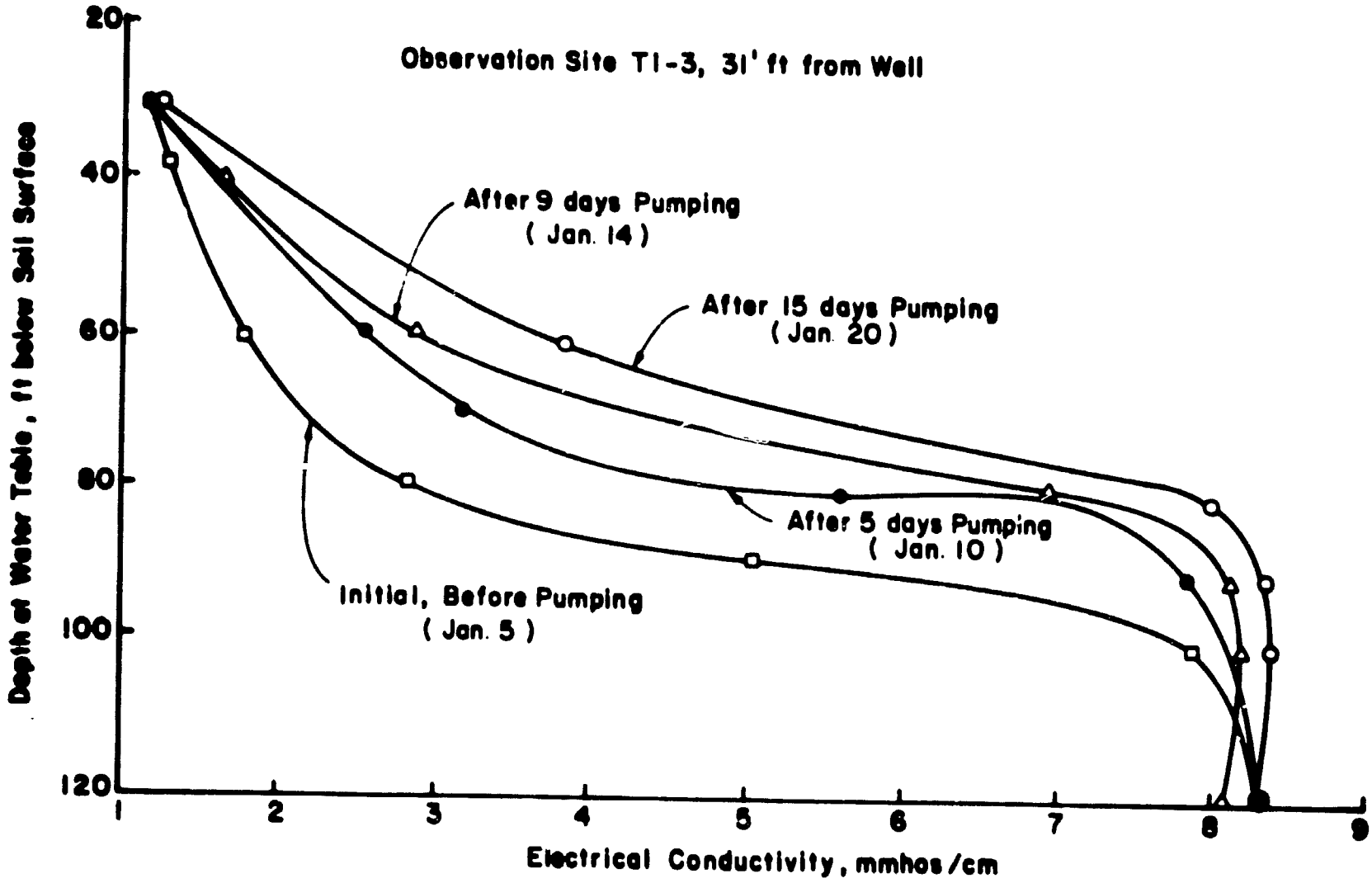

Figure 23. Salinity of water in the aquifer as a function of depth below the surface and before and during pumping.

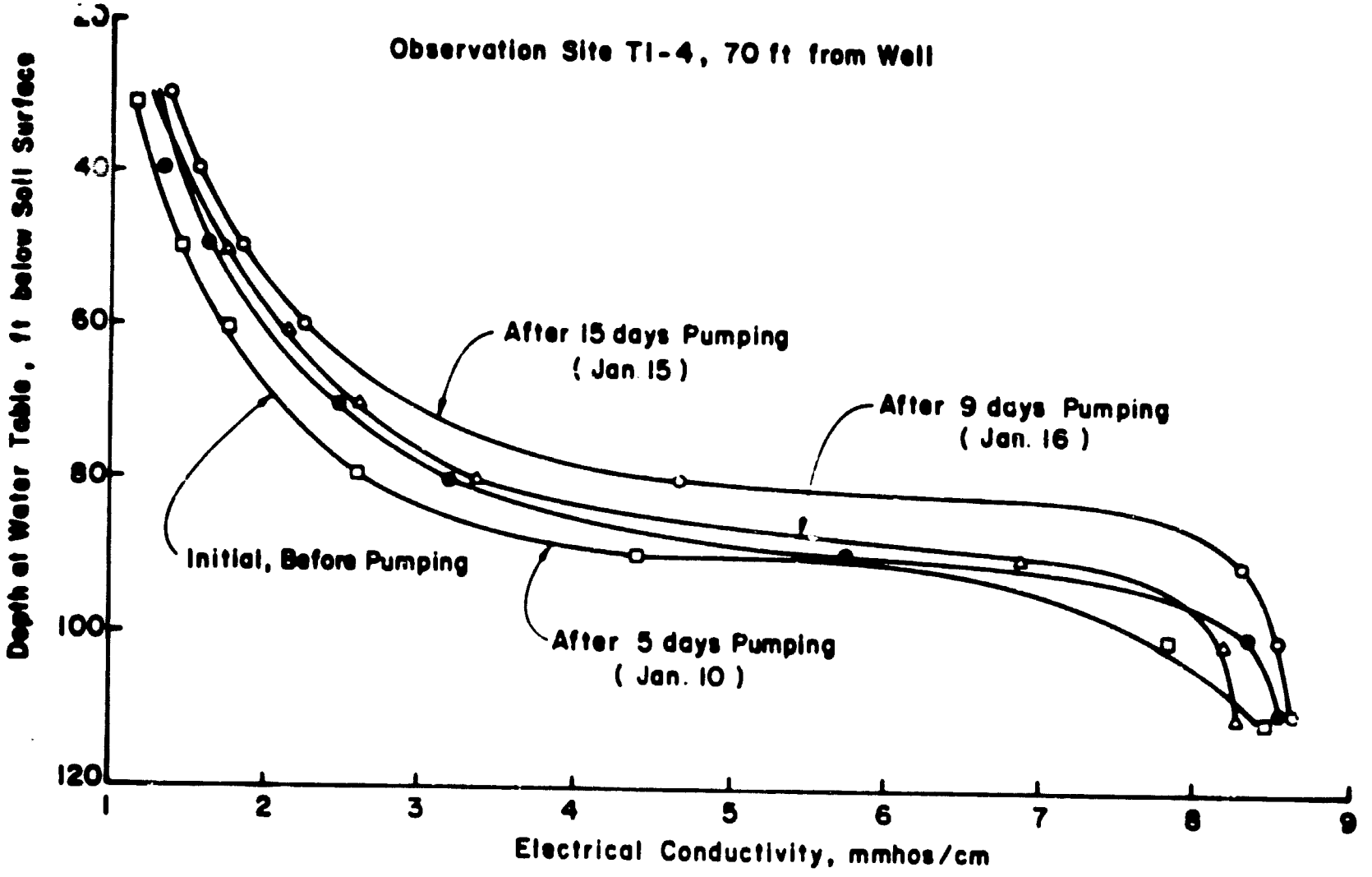

Figure 24. Salinity of water in the aquifer as a function of depth below surface before and during pumping.

fresh and the saline waters. Plotting the 5 mmhos/cm concentration line as a function of depth and distance from the well before and during pumping illustrates the rise of the salire-fresh water interface in Figure 25. At the center of Figure 25 the well is illustrated as it extends to 60 feet below the surface with the wellscreen or filter section being from 10 to 60 feet below the surface.

The concentration of the pumped water is illustrated in Figure 26. Again, the variations in temperature caused some scatter from the curve during the measurements prior to January 14; however, after the 14th there was a very consistent rise in concentration with time. Pumping was discontinued on the 20th because the salinity of the water was becoming so high that it was not acceptable for irrigation. At this time, the 5 mmhos/cm concentration surface had reached the bottom of the well and the lower portion of the well was exposed to water of concentration higher than the initial values.

The well was turned off on January 20 and the cone of saline water began to recede. The position of the cone during recession is shown in Figure 27. Again, the rate of recession is much less than the rate of rise.

The degree of penetration of tubewell 2 and the discharge rate were purposely made larger than all of the theoretical calculations indicated for optimum conditions. This was done to insure that substantial coning would indeed occur during the tests. Comparisons of the degree of upconing

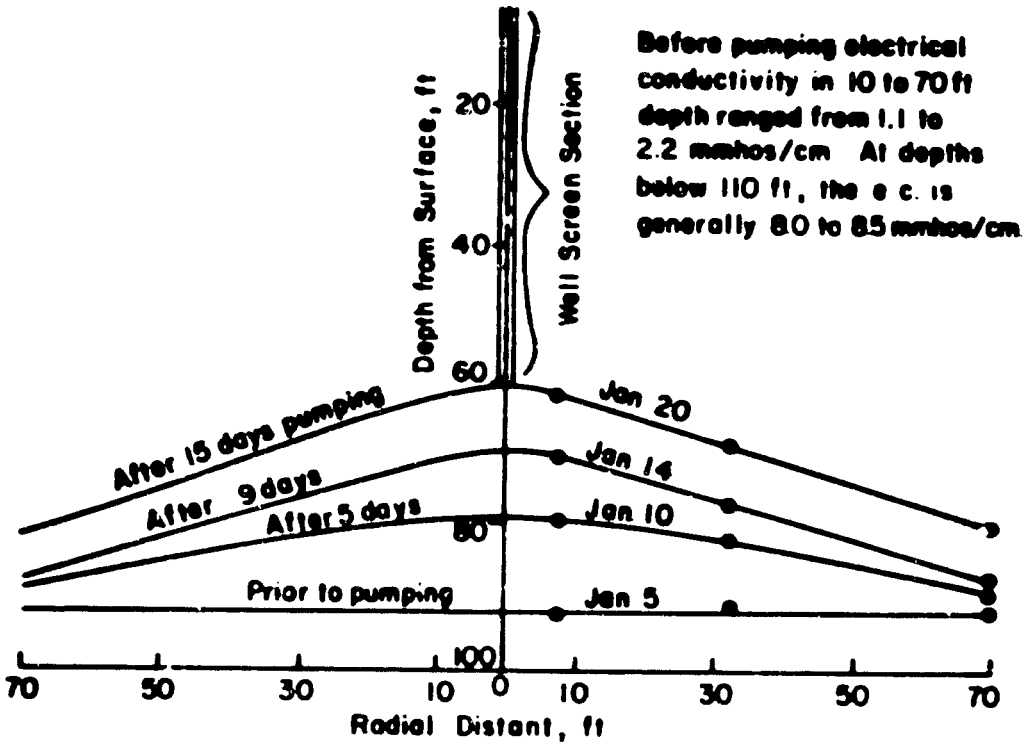

Figure 25. Rise of saline-fresh water interface as indicated by the successive positions of the 5 mmho/cm isoconcentration line.

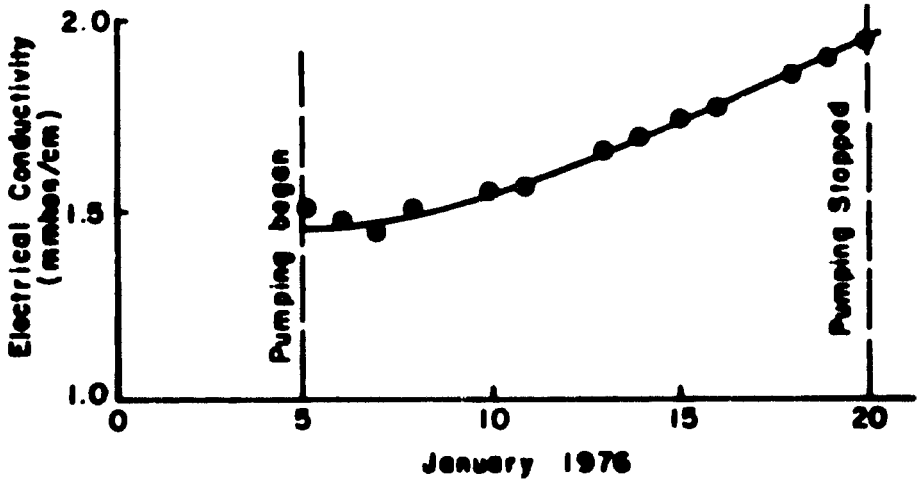

Figure 26. Salt content of well water which was being pumped at a rate of 225 gallons/minute.

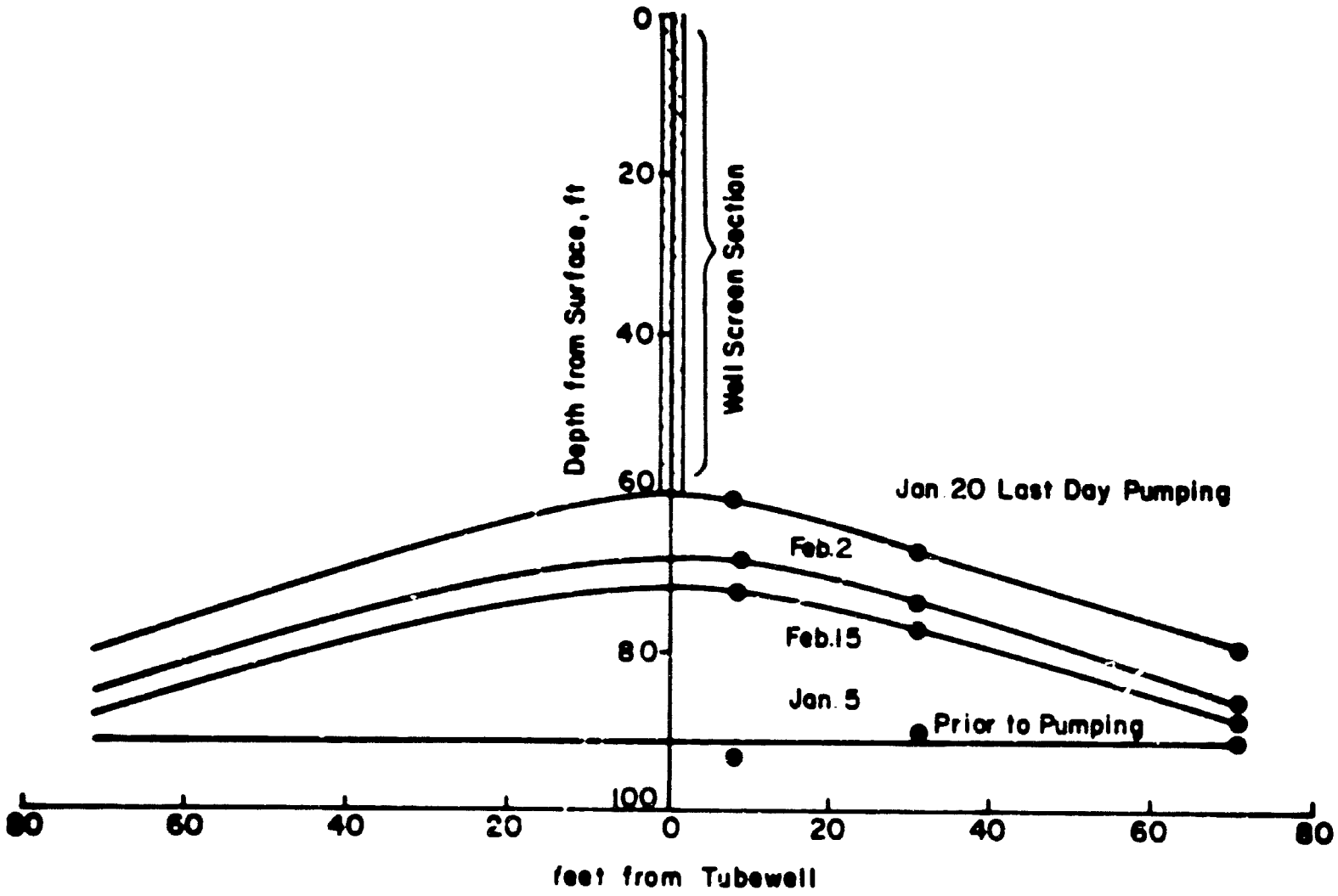

Figure 27. Fall of saline-fresh water interface following pumping (as indicated by successive positions of 5 mmhos/cm equal concentration line).

beneath tubewells 1 and 2 clearly show that too much penetration and too large a discharge will cause a significant decline in the quality of the pumped water as predicted by the theoretical computations. Specifically, tubewell 1, penetrating only 30 percent of the fresh water zone and pumped at 65 gpm for 13 days, produced only about 8 ft. of upconing beneath the well. This is to be compared with tubewell 2 which penetrates 60 percent of the fresh water layer and was pumped at 225 gpm for 15 days to produce an upconing in excess of 30 ft. The construction and operation of tubewell 1 (relative to penetration and discharge) was selected based on the theoretical predictions. Therefore, the field tests produced a qualitative validation of the theoretical results.

All of the theoretical models reported herein require knowledge of the hydraulic properties of the aquifer. The results of the field tests and other field observations (McWhorter, 1975) suggest a simpler approach to upconing calculations that do not require the hydraulic parameters. Laboratory results, theoretical considerations, and field observations suggest that the shape of the interface is given approximately by

$$\xi = C \ln r_e/r$$

where ξ is the height of the interface above its horizontal equilibrium position, C is a constant, r = distance from the pumped well and r_e is the radius of influence. Therefore, the volume of fresh water displaced by the rising interface is

$$V = 2\pi CSy \int_{r_w}^{r_e} \xi \, dr$$

$$= \pi CSy \left\{ \frac{r_e^2}{2} - \frac{r_w^2}{2} - r_w^2 \ln r_e/r_w \right\}$$

where V is the volume of fresh water displaced, Sy is the specific yield of the aquifer, and r_w is the effective radius of the pumped well.

Reasonable value of r_w, r_e, and Sy for Pakistan are 1 ft., 500 ft., 0.25, respectively. Thus,

$$V = 9.81 \times 10^4 \, C$$

and the height of the interface beneath the well as a function of the volume displaced becomes

$$\xi_w = 6.3 \times 10^{-5} \, V$$

where ξ_w is the height of the interface beneath the well in feet and V is the displaced volume in cubic feet. Comparison of interface heights calculated from the above equation with those measured in both field experiments agree reasonably well. This comparison was made by assuming the entire volume of pumped water was displaced by the upconed interface (i.e., V = Q tp, where Q is discharge and tp is the pumping time). This procedure results in predicted upconing that is conservatively large.

It is not expected that the above simple theory would hold at large pumping times when the interface tends to stabilize. In most practical situations, continuous pumping periods will probably be on the order of those utilized in the experiments and the above computations should be reasonably accurate up to 15 days of continuous pumping.

Before proceeding to a discussion of guidelines for the construction and operation of skimming wells it is worth reporting the successful modification of an existing well to conform more closely with the characteristics of a skimming well. A small tubewell, located on the Phularwan Research Farm (a part of the Mona Reclamation area), was constructed to a depth of 105 feet, during 1974. The discharge from this well contained 2300 ppm dissolved solids with an SAR of about 14. Use of water from this well had been discontinued for about two months because of the high salinity. An investigation disclosed the salinity profile presented in Table 5.

Table 5. Salinity Profile in Mona Well on Phularwan Farm.

Depth ft.	Elec. Cond. mmohs/cm
13-23	2.10
23-33	1.96
33-43	1.75
43-53	1.47
53-63	1.30
63-73	1.20
73-83	1.20
83-93	1.96
93-103	3.75

These data indicate a relatively fresh water zone (800 ppm) above a more saline zone (greater than 2500 ppm) with a transition zone located below about 90 feet. Water from a nearby hand pump indicated that the relatively high conductivities measured in the first 40 feet of the well casing resulted from more saline water pumped from below during the

last period of pump operation. Since the top 30 feet of the well was cased with blind pipe, water in this section would come to equilibrium with the natural ground water salt content very slowly and this is probably the reason for the somewhat higher salt content.

Based on the above observations, it was recommended that the tubewell be modified by blocking off the bottom 45 feet with sand and a concrete plug. This was accomplished leaving the well with blank casing from the surface to about 30 feet and well strainer from 30 to 60 feet. A flange with a small orifice was inserted in the discharge pipe which decreased the pumping rate to 180 gpm from the original 400 gpm. These modifications resulted in the marked improvement in the pumped water as indicated in Table 6.

Table 6. Salinity in Discharge - Mona Well on Phularwan Farm

Time of Pumping	Total Salts (ppm)	Sodium Adsorption Ratio	Pumping Rate (cusecs)
Prior to modification	2300	14	0.9
Following modification			
1 min. of pumping	830	3.6	0.4
20 min. of pumping	850	3.6	0.4
160 min. of pumping	770	3.3	0.4
One month later			
4 hours of pumping	830		0.4

The water from this well is now used regularly for irrigation on the research station.

CONSTRUCTION AND OPERATION OF SKIMMING WELLS

As a result of the laboratory and theoretical model studies and the field experiments, several recommendations relative to the design and operation of skimming wells can be made. No specific design details are recommended for the construction of skimming wells; rather design criteria are recommended which can be satisfied by a number of specific designs. Ideally, the hydraulic parameters of the aquifer at the specific location where the skimming facility is contemplated should be determined and one of the mathematical models used to provide specific design and operation criteria. It is realized that such a procedure would require financial and technical resources beyond that which are usually available. Therefore, the guidelines presented in this section were developed so that such information is not required. The associated loss in rigor and physical realism is not believed to compromise the validity and utility of the guidelines.

Construction

1) The salinity profile should be established as a first step so that the thickness of the "fresh" water layer can be estimated. The salinity profile can be established by measuring the EC of water in a pilot bore hole or in an existing well in the immediate vicinity. If an existing well is used, credence should be given only those readings taken within the screened portion following a 4-5 day period of no pumping.

2) The skimming well should be constructed so that the screened portion is located in the upper part of the fresh-water zone. If during boring, no significant layering is noted, the length of well screen or strainer should be about 30 percent of the thickness of the "fresh" water zone. If there is evidence that the vertical permeability is substantially less than the horizontal permeability (e.g. if stratification exists) the length of screen or strainer can be extended to about 50 percent of the thickness of the fresh water zone.

3) If a clay lens or other tight layer is encountered within the fresh water zone, consideration should be given to screening only the portion of the well above the tight layer. This procedure will assist in controlling the upconing of salt water from below. If the tight layer has been penetrated by the bore, all hole below the layer should be carefully backfilled to prevent the bore from providing a "short-circuit".

4) Every effort should be made to minimize well losses by good well construction practices. While large well losses will not increase upconing, they may cause the discharge to be limited to values below that which could be safely pumped.

Operation

The following guidelines for operation of a skimming well are based on limiting the total volume pumped rather than rate of pumping. If sustained pumping is desired at

very low rates, more volume may be pumped during a single pumping period than is indicated below.

1) Significant salt water entrainment should not occur if the interface beneath the well does not rise beyond one-half the distance between the undisturbed interface and the bottom of the well. Let H_e be the initial thickness of the fresh water zone and d be the length of screen or strainer. As indicated previously, d/H_e should be between 0.3 and 0.5. The maximum safe rise of the interface is $0.5\ (H_e - d)$. Therefore, the maximum volume that can be pumped safely during a single pumping period is

$$V = 8 \times 10^3\ (H_e - d)$$

where V is in cubic feet and H_e and d are expressed in ft. This criterion allows for a combination of pumping rates and durations to meet specific requirements.

As an example, suppose it was desired to pump tubewell 2 at 0.5 ft^3/s. How long can this rate be sustained safely? In the case of tubewell 2, $H_e - d = 31$ ft. Thus, a total volume of $2.48 \times 10^5\ ft^3$ can be pumped before salt water entrainment becomes a danger. At a rate of 0.5 ft^3/s, the maximum pumping time is 4.96×10^5 seconds or about 6 days. At a rate of 0.25 ft^3/s, the pumping

duration could be at least 12 days. In the case of tubewell 1, for which $H_e - d = 60$ ft., a total volume of 4.8×10^5 ft^3 could be pumped safely. The above guideline dictates a pumping period of 38 days at a rate of 65 gpm (0.14 ft^3/s). Indeed, the field experiments resulted in about 8 ft. of upconing after 13 days of pumping.

2) It is recommended that the rest period between pumping periods be about 5 times the length of the pumping period. For highly permeable aquifers, the recession of the interface may be more rapid than this guideline indicates. Significant vertical recharge may also cause the interface to recede more rapidly.

REFERENCES

Chandler, R.L. 1973. Salt Water Coning in Anisotropic Media. Unpublished M.S. Thesis, Department of Agricultural Engineering, Colorado State University, Fort Collins, CO.

Chandler, R.L. and McWhorter, D.B. 1975. Interface Upconing Beneath a Pumping Well. Ground Water, Vol. 13, No. 4, p 354-359.

Dagan, G. 1971. Perturbation Solutions of the Dispersion Equation in Porous Mediums. WRR, Vol. 7, No. 1, p. 135-142.

Dagan, G. 1964. Second Order Linearlized Theory of Free Surface Flow in Porous Media. La Houille Blanche, No. 8, p. 901-910.

Greenman, D.W., Swarzenski, W.V. and Bennett, G.E. 1967. Groundwater Hydrology of the Punjab, West Pakistan with Emphasis on Problems Caused by Canal Irrigation. U.S. Geological Survey Water Supply Paper 1608-H.

Hantush, M.S. 1968. Unsteady Movement of Fresh Water in Thick Unconfined Saline Aquifers. Bull. Intern. Assoc. of Sci. Hydrology, Vol. 13, No. 2, p. 40-60.

Harleman, D.R.F. and Rumer, R.R., Jr. 1963. Longitudinal and Lateral Dispersion in an Isotropic Porous Medium, Journal of Fluid Mechanics, Vol. 16, Part 3, p. 38[illegible]-394.

Lapidus, L. and Amundson, N.R. 1952. Mathematics of Adsorption in Beds VI: The Effect of Longitudinal Diffusion in Ion Exchange and Chromatographic Columns. Journal of Physical Chemistry, Vol. 56, p. 984-988.

Lindstrom, R.T., Boersma, L. and Stockard, D. 1971. A Theory on the Mass Transport of Previously Distributed Chemicals in a Water Saturated Sorbing Porous Medium: Isothermal Cases, Soil Science, Vol. 112, No. 5.

McWhorter, D.B. 1975. Water Supply for Irrigation on Andros Island, Bahamas. Trip report to Western Institute for Science and Technology and to Water Management Research Project, Colorado State University.

McWhorter, D.B. 1972. Steady and Unsteady Flow of Fresh Water in Saline Aquifers. Water Management Tech. Report No. 20, Colorado State University, Fort Collins, CO.

Muskat, M. and Wyckoff, R.D. 1935. An Approximate Theory of Water-Coning in Oil Production. AIME, Trans., Vol. 114, p. 144-163.

Muskat, M. 1965. Flow of Homogeneous Fluids. J.W. Edwards, Ann Arbor, Michigan.

Ogata, A. 1964. Mathematics of Dispersion with Linear Adsorption Isotherm, Prof. Paper 411-H, U.S Geological Survey, U.S. Government Printing Office, Washington, D.C. 9 p.

Ogata, A. and Banks, R.B. 1961. A Solution of the Differential Equation of Longitudinal Dispersion in Porous Media, Prof. Paper 411-A, USGS, U.S. Government Printing Office, Washington, D.C. 7 p.

Sahni, B.M. 1972. Salt Water Coning Beneath Fresh Water Wells. Unpublished Ph.D. Dissertation, Department of Agricultural Engineering, Colorado State University, Fort Collins, Colorado.

Wang, F.C. 1965. Approximate Theory for Skimming Well Formulation in the Indus Plain of West Pakistan. Journal of Geoph. Res., Vol. 70, No. 20, p. 5055-5063.